Food Hydrocolloids 150 (2024) 109728

Contents lists available at ScienceDirect

Food Hydrocolloids

journal homepage: www.elsevier.com/locate/foodhyd

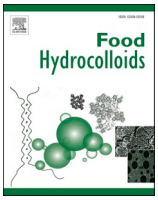

Composition, characterisation and emulsifying properties of natural nanoparticles in chickpea aquafaba for the formation of chilli oleoresin-in-water Pickering emulsions

S.S. Sahin, A.J. Hernández-Álvarez **, L. Ke, A. Sadeghpour, P. Ho, F.M. Goycoolea *

School of Food Science and Nutrition, University of Leeds, Leeds, LS2 9JT, United Kingdom

ARTICLE INFO

Keywords:
Aquafaba
Chickpea
Encapsulation
Nanoparticle
Chilli oleoresin
Capsaicin

ABSTRACT

This study aims to assess the compositional characteristics of British Kabuli chickpea aquafaba (AF) by conducting a comprehensive analysis from raw chickpeas to centrifugation fractions of AF and its potential use in forming and stabilising capsaicin-loaded O/W Pickering systems by exploiting the presence of self-assembled nanoparticles and proteins, which act as natural-coating agent. To this end, chickpeas were soaked (16 h, 4 °C, 1:4 chickpea: water) and pressure-cooked (20 min, 113 °C, 10 psig, 1:5 chickpea: water). The dry weight-based (DWB) compositions included total carbohydrate (76.33 ± 4.20%), protein (16.29 ± 0.43%), total phenolics (7.05–8.77 mg/g) and saponins (39.95 ± 0.89 mg/g), thus confirming the leaching of these components from seeds to AF. SDS-PAGE electrophoresis analysis revealed the presence of low MW proteins (≤~16 kDa). The monosaccharides comprised D-glucose, D-galactose, L-arabinose, D-xylose and D-fructose. AF's particle size distribution revealed the occurrence of a bimodal population of nanoparticles (D_h ≤~1000 nm and D_h ≤~100 nm), further characterised by SAXS and TEM imaging. O/W emulsions were prepared with three chilli oleoresin types (capsicum, chilli birds' eye, and chilli ancho) by high-pressure homogenisation. The emulsion with the highest capsaicin content (capsicum oleoresin) was the most stable while the emulsion with the lowest capsaicin content (chilli ancho oleoresin) was the least stable. The presence of incidental nanoparticles and denatured proteins in AF was reasoned to account for the formation and stabilisation of chilli oleoresin-in-water Pickering emulsions, a newly offered explanation for its interfacial properties that will be pursued further in future studies.

1. Introduction

The demand for plant-based foods has increased drastically over the past decade due to the increasing trend of vegan diets worldwide (Kumar et al., 2022). Aquafaba (AF), the broth obtained from cooking chickpeas (*Cicer arietinum* L.) in water at high temperatures, is regarded as a waste liquid stream during their industrial canning process. The term 'aquafaba' (AF) originates from the Latin words, *aqua* (water) and *faba* (beans) (The Official Aquafaba Website, 2016). During boiling, it is known that the legume components undergo structural transformations caused by heat treatment (Shevkani, Singh, Chen, Kaur, & Yu, 2019). These include leakage of different components from the seeds into the boiling water. As a result, AF has been found to exhibit beneficial techno-functional properties such as foaming, emulsifying and thickening (Mustafa, He, Shim, & Reaney, 2018). Based on this, AF has been studied as a replacement for animal-based additives like egg white in food formulations such as mayonnaise (He, Purdy, et al., 2021), meringues (Meurer, de Souza, & Marczak, 2020), cakes (Karatay, Rebellato, Joy Steel, & Dupas Hubinger, 2022) ice cream and cheese (He, Meda, Reaney, & Mustafa, 2021). However, its use as a wall material to encapsulate bioactive compounds such as capsaicin has not been investigated yet.

The process of boiling daily foods is known to lead to the formation of incidental nanoparticles, such as porcine bone soup (Gao et al., 2021), black tea infusion (Han et al., 2022) and green tea extract nanoparticles (Gopal, Muthu, Paul, Kim, & Chun, 2016). Additionally, self-assembled particles like licorice protein nanoparticles have been demonstrated the potential to encapsulate poisonous alkaloids and mitigate their toxicity (Ke, Gao, Shen, Zhou, & Rao, 2015). To the best of our knowledge, the formation of incidental nanoparticles in AF during chickpea or other

* Corresponding author.
** Corresponding author.
E-mail addresses: a.j.hernandezalvarez@leeds.ac.uk (A.J. Hernández-Álvarez), f.m.goycoolea@leeds.ac.uk (F.M. Goycoolea).

https://doi.org/10.1016/j.foodhyd.2024.109728
Received 28 October 2023; Received in revised form 26 December 2023; Accepted 2 January 2024
Available online 4 January 2024

legume cooking has not been documented. The interfacial behaviour of these nanoparticles can be leveraged in the Pickering stabilisation of emulsions by AF. Evidence of their occurrence and characteristics offer a renewed interpretation of the colloidal interfacial activity of AF. Pickering emulsions are stabilised by the adsorption of small solid nanoparticles at the oil-water interface, instead of surfactants. These systems have been the subject of extensive studies as recently reviewed by Sarkar and Dickinson (2020) and studied by Zhao, Wang, Xiao, Chen, and Cao (2020) and Liu and Tang (2016). The application of these systems includes the encapsulation of bioactive substances such as chilli capsaicinoids as we show in the present study.

Capsaicin (8-methyl-*N*-vanillyl-6-nonenamide) is the main active agent and secondary alkaloid present in chilli pepper (*Capsicum annum*) and is widely used in the food and pharmaceutical industry applications (Kaiser, Higuera, & Goycoolea, 2017). Along with dihydrocapsaicin, capsaicin is the most common member of the capsaicinoids family and has lipophilic, colourless and odourless properties. Pharmacological applications of capsaicin extend beyond pain relief treatments. Approved for topical use in pain management, this natural compound has also garnered attention for its diverse bioactivities including cholesterol-lowering, anti-inflammatory, anti-cancer, anti-obesity and antioxidant properties (Guzmán & Bosland, 2018). Considering the toxic nature, pungency and lack of user-friendly properties associated with pure capsaicin, natural extraction products and oleoresin forms are predominantly preferred in food formulation (Akbas, Soyler, & Oztop, 2019). Chilli oleoresins are viscous liquid or semi-solid substances obtained by extracting their source's fragrance and flavour from finely ground chilli powder (Peter & Babu, 2012). Food formulations are characterised by a high proportion of water which compromises the functionality of capsaicin given its low solubility. For this reason, capsaicin encapsulation systems can improve not only its delivery properties but also its stability, bioaccessibility and effectiveness, as shown in previous studies by Kaiser et al. (2015, 2016) and da Silva Anthero, Moya, Torsoni, Cazarin, and Hubinger (2022).

Although the techno-functional properties of AF have been extensively documented (Crawford, Kerr, & Tyl, 2023; He, Shim, Mustafa, Meda, & Reaney, 2019; Karatay et al., 2022), its utilisation as a coating agent or wall material in the encapsulation of bioactive compounds such as chilly capsaicinoids via the formation and stabilisation of Pickering oil-in-water emulsions by incidental nanoparticles and unfolded proteins leached during cooking, has not yet been investigated. In our study, we investigated compositional and techno-functional colloidal properties of AF obtained from British Kabuli chickpeas with a focus on the formation, properties and stability of chilli oleoresin-loaded emulsions systems.

2. Materials

British Kabuli chickpeas (*Cicer arietinum* L.) were purchased from Hodmedod's Company, UK and they were stored at room temperature in a dry environment. Desi chickpeas were bought from a local market in Santa María del Páramo, León, Spain. Capsicum, chilli ancho and chilli birds' eye oleoresins were kindly donated by Lionel Hitchen Ltd. Capsaicin (≥95%), phenol (≥95%), sulfuric acid (≥99%), D-glucose, L-rhamnose monohydrate, L-arabinose, D-fructose, D-glucuronic acid, sodium phosphate monobasic monohydrate, Folin-Ciocalteu phenol reagent, Fast Blue BB hemi (zinc chloride) salt, formic acid, acetonitrile (HPLC grade), methanol (≥99%), *m*-hydroxyphenyl, gallic acid sodium tetraborate decahydrate were purchased from Sigma-Aldrich Ltd (Massachusetts, USA). Trifluoracetic acid (≥99%), D-galactose, D-xylose, sodium hydroxide, dithiothreitol, and sodium carbonate anhydrous were provided from Thermo Fisher Scientific (Cleveland, OH, USA). Vanillin was purchased from Glentham Life Sciences (Wiltshire, UK) and diosgenin was provided from Fluorochem (Hadfield, UK).

3. Methods

3.1. Aquafaba production

Chickpeas were soaked with 1:4 (w/v) seed:distilled water ratio at 4 °C for 16 h and then the soaking water was drained and discarded. Soaked chickpeas (SC) were cooked with 1:5 (w/v) chickpea:distilled water ratio (CWR) at 113 °C and 10 psig for 20 min in the pressure cooker. In preliminary studies, it was found that while the British Kabuli's AF material had microparticles of average hydrodynamic diameter (D_h) of 612 ± 16 nm, Desi's AF had more than twice as large particles (1740 ± 187 nm). Based on these results, as well as the lack of studies on AF properties of British Kabuli, we decided to keep the focus only on this variety for a further comprehensive analysis. To see the varieties between supernatant (SP) and pellet (P), AF centrifugation (Heraeus Fresco 21; Thermo Scientific, USA) at 14,800 rpm, 25 °C for 40 min was applied. A total of 0.02% sodium azide was added to uncentrifuged AF, SP and P as a preservative during storage at 4 °C for further analysis. AF, SP and P were freeze-dried (Labconco, Kansas City, MO, USA) at −55 °C for 48 h for compositional analysis. The measured pH of the freshly produced AF was ~5.84.

3.2. Characterisation of British Kabuli Chickpea aquafaba

3.2.1. Dry matter content

The dry matter content (%) of AF was determined quantitatively based on the gravimetric loss of free water from the AF medium while freeze-drying at −55 °C for 48 h. The liquid AF was dried until the sample mass stabilised and the dry matter content was calculated with the ratio of dry AF to the initial mass of liquid AF.

3.2.2. Total carbohydrate analysis

The total carbohydrate (%) of raw British Kabuli chickpea seed (RC), soaked chickpea (SC), cooked chickpea (CC), aquafaba (AF), supernatant (SP) and pellet (P) were determined based on the phenol-sulfuric acid colourimetric test by the method of Dubois, Gilles, Hamilton, Rebers, and Smith (1956) with slight modifications. RC, SC and CC were hydrolysed with acid prior to total carbohydrate assay. To this end, SC and CC were freeze-dried at −55 °C for 24 h. Afterwards, these samples and raw chickpeas were ground into powder, and 0.1 g of the powder was hydrolysed in a boiling water bath for 2 h with 5 mL of 6 N HCl. After cooling to room temperature, it was neutralised with around 3 g of Na_2CO_3 until the effervescence ceased, centrifuged at 5000 rpm for 10 min and the supernatant was collected for the total carbohydrate analysis. AF and SP were used directly in liquid form and the P was resuspended in the same volume of distilled water. An aliquot of 42 μL was placed in a 96-well microplate, then a 42 μL aliquot of a freshly prepared phenol aqueous solution (5%) was added, followed by the addition of 216 μL of concentrated sulfuric acid. The plate was kept at room temperature for 20 min and the absorbance at 490 nm was read on a spectrophotometric plate reader (Spark 10 M, Tecan Group Ltd, Zürich, Switzerland). Blanks were run with Milli-Q water. A standard curve (R^2 = 0.99) of D-glucose is prepared with Milli-Q water in the range of 10–150 μg/mL.

3.2.3. Monosaccharides composition

Monosaccharide composition of AF, SP and P were observed by using high-performance anion-exchange chromatography with pulsed-amperometric detection (HPAEC-PAD) (Dionex, Idstein, Germany) which takes advantage of the anionic properties of neutral carbohydrates at high pH (>12) (Xie et al., 2013). The system is equipped with Dionex CarboPac™ PA20 Analytical, 3 × 150 mm (P/N 060,142) column operated at 0.4 mL/min flow rate at 25 °C and the sample injection volume was 10 μL. Milli-Q water and 300 mM NaOH were used as eluents in the system. Prior to HPAEC-PAD characterisation, acid hydrolysis of the polysaccharides in the sample composition is essential. To achieve

this, the method of López-Franco et al. (2008) was used. Briefly, 1 mg of the sample was transferred to 1 mL of 2 M TFA (trifluoroacetic acid). The mixture was then placed in a boiling water bath (~100 °C) to hydrolyse for 4.5 h and cooled to room temperature. To evaporate TFA, tubes were kept in the nitrogen evaporator at 40 °C until only dry residue remained. The contents were redissolved in 1 mL of ultra-pure water. The aliquot was filtered through a 0.45 μm nylon syringe filter (Gilson, UK) and taken into vials for HPAEC-PAD analysis. Sugar standards (10 μg/mL) were prepared in ultra-pure water. The HPAEC gradient used for the detection of monosaccharides is shown in Suppl. Table 1.

3.2.4. Uronic acid content

Uronic acid content (%) was measured according to the colourimetric protocol of Blumenkrantz and Asboe-Hansen (1973) with minor adjustments. AF and SP were used in liquid form and the P was resuspended in the same volume of water. 0.2 mL of samples were added to glass tubes, and they were cooled in an ice bath. An aliquot of 1.2 mL sodium tetraborate in H_2SO_4 solution (0.0125 M) was added to tubes and they were vortexed vigorously. The tubes were then heated in a boiling water bath for 5 min and immediately placed in the ice bath. Subsequently, 0.20 μL of 0.15% *m*-hydroxydiphenyl was added. Tubes were vortexed again and kept at room temperature for 20 min. Afterwards, an aliquot of 300 μL of each sample from the tubes is transferred to the 96-well microtiter plate. Absorbances were recorded at λ = 520 nm using the spectrophotometric plate reader. Standard curve (R^2 = 0.99) was prepared by D-glucuronic acid (0–75 μg/mL) in Milli-Q water.

3.2.5. Elemental analysis and protein content

Carbon (C), hydrogen (H) and nitrogen (N) content (%) of RC, SC, CC, AF, SP and P were measured by using an elemental analyser located in the School of Geography, University of Leeds. Freeze-dried samples were used. Rice flour and EDTA were used as standards. The protein content (%) of samples was calculated by multiplying the nitrogen content by 6.25.

3.2.6. SDS-PAGE analysis

Electrophoretic separation of RC, SC, CC, AF, SP and P was performed based on sodium dodecyl sulfate-polyacrylamide gel electrophoresis (SDS-PAGE) protocol which is suggested by Laemmli (1970). Both reducing and non-reducing conditions were applied. 3 mg of freeze-dried samples were diluted with 0.25 mL of 1*X* Laemmli sample buffer and boiled at 95 °C for 10 min in a heating block. Afterwards, the sample tubes were centrifuged at 10,000 rpm, 4 °C for 10 min 20 μg of protein (samples) and 10 μL of Precision Plus Protein standards (BIO--RAD, Berkley, CA, USA) were loaded per well onto Criterion AnyKD TGX gel (BIO-RAD, Berkley, CA, USA). Mini-PROTEAN Tetra cell system (BIO-RAD, Berkley, CA, USA) was used for electrophoresis and proteins were separated at 200 V for 35 min. Subsequently, the gel was washed three times for 5 min each in 200 mL of Milli-Q water and shaken overnight in 50 mL of Bio-Safe Coomassie Stain (BIO-RAD, Berkley, CA, USA). The gel image was analysed by using the ChemiDoc XRS + Gel Imaging System (BIO-RAD, Berkley, CA, USA).

3.2.7. Saponins content

Saponins quantification (mg/g) of RC, SC, CC, AF, SP and P was conducted following the method of Sánchez-Velázquez et al. (2021). For the saponins extraction, 0.5 g of RC and freeze-dried samples (SC, CC, AF, SP and P) were weighed into tubes. 10 mL of 80% (v/v) methanol in water was added and vortexed. The tubes were agitated for 16 h. Afterwards, they were centrifuged at 5000 rpm for 10 min and the supernatant was collected. Five mL of 80% (v/v) methanol was added into tubes and subsequently, centrifuged at 5000 rpm for 10 min. This step was repeated twice, and all supernatants were pooled together. 200 μL of this extract is mixed with 50 μL of 80% methanol. Afterwards, tubes were transferred to an ice bath followed by the addition of 0.25 mL of vanillin reagent (80 mg/mL in methanol) and 2.5 mL of 72% sulfuric acid. Tubes were vortexed and kept in the water bath at 60 °C for 10 min. The absorbances of the samples were read at λ = 520 nm against the Milli-Q water as blank. Saponin contents were calculated using a diosgenin (0–125 μg/mL) calibration curve (R^2 = 0.99).

3.2.8. Total phenolics content

The total phenolics content (mg/g) was determined based on the method of Pico, Pismag, Laudouze, and Martinez (2020) with slight modifications by using both Folin-Ciocalteu and Fast Blue BB assays. First, to collect the total extractable phenolic compounds (EPP), 1 g of the samples were solubilised in 12 mL of 80% methanol in 0.1% formic acid. Tubes were agitated for 15 min and centrifuged for 5 min at 3500 rpm at room temperature. The supernatants were collected and 12 mL of 70% acetone in 0.1% formic acid was added to pellets for the second extraction using the same conditions as above. Supernatants were combined and 40 μL of EDTA (2%) was added to stabilise flavon-3-ols. 12 mL of EPP extracts were kept for Folin-Ciocalteu and Fast Blue BB analysis as a control group without interference removal while the rest 12 mL was treated with solid phase extraction (SPE) to remove the polar substances from EPP. For SPE, Oasis HLB 1 cc (30 mg) cartridges were used. Cartridges were firstly activated by 3 mL of 1% formic acid in methanol and secondly 3 mL of 1% formic acid in water into the waste tubes. Tubes were changed and 3 mL of EPP was eluted into new SPE tubes. Again, tubes were changed to waste and the polar interferences were washed by using 1 mL of 0.05 M NaH_2PO_4. Subsequently, 3 mL of 0.1% formic acid in methanol was eluted and collected into the SPE tubes. These tubes were kept at −80 °C for further analysis. Afterwards, Folin-Ciocalteu and Fast Blue BB assays were applied for both EPP and SPE samples. Gallic acid (0–500 μg/mL) was used as a standard for both methods.

Folin-Ciocalteu method (Singleton, Orthofer, & Lamuela-Raventós, 1999) was conducted by pipetting 10 μL of standard/EPP/SPE, 40 μL of Folin-Ciocalteu reagent and 150 μL of 4% Na_2CO_3 in a 96 well-plate, respectively. The sample was incubated for 30 min in the dark and the absorbance was measured at λ = 756 nm.

Fast Blue BB technique (Pico et al., 2020) was applied by mixing 200 μL of standard/EPP/SPE, 20 μL of 0.1% Fast Blue BB reagent and 20 μL of 5% NaOH into a 96 well-plate and incubated for 2 h in the dark. The absorbance was read at λ = 420 nm.

3.3. Biophysical characterisation of aquafaba nanoparticles

3.3.1. Small-angle X-ray scattering (SAXS)

Small-Angle X-ray Scattering (SAXS) measurements were conducted to investigate the size (radius of gyration, R_g) and shape of putative self-assembled aquafaba nanoparticles, and of any other occurring dissolved nanometric components (*e.g.*, macromolecular species). We used a SAXSpace camera (Anton Paar, Austria) equipped with a line collimation system providing a Cu-K_α radiation beam with λ = 0.154 nm wavelength and a mythen 1D detector (Dectris, Switzerland). Measurements were conducted under the high-resolution mode, enabling the detection of the minimum scattering vector, $q_{min} = 0.12\ nm^{-1}$ ($q = (4\pi/\lambda)sin\ (\theta/2)$), where θ is the total scattering angle. All samples were placed inside an identical, vacuum-sealed 1.5 mm quartz capillary, ensuring uniform scattering volume and background intensities for all measurements. All measurements including empty capillary and solvent were conducted for 40 min. The sample temperature was equilibrated at 25 °C. The scattering data was transmission-corrected by normalising the attenuated scattering intensity at $q = 0$ to unity. The scattering patterns were corrected owing to the primary beam position by using SAXStreat Software (Anton Paar, Austria) and the background subtracted on SAXSquant software (Anton Paar, Austria). In order to interpret the scattering profiles of the AF sample, two explanations have been proposed based on: i) scattering from potential self-assembled nanoparticles and ii) scattering from swollen chains formed by unfolded proteins. For particle scattering, the Indirect Fourier

Transformation (IFT) (Bergmann, Fritz, & Glatter, 2000; Glatter, 1977) approach was applied to simulate the scattering curves and obtain their corresponding Pair-Distance Distribution Functions (PDDF) and radii of gyration (R_g). This analysis was performed using GIFT software (University of Graz, Austria) while the maximum dimension in real-space was determined by the instrumental resolution where the minimum scattering vector modulus was recorded ($q_{min} = 0.15\ nm^{-1}$). The data interpretation based on the swollen chain (unfolded proteins) scattering in solution mainly relies on the power law scattering intensities. Further details are described in Results and Discussions.

3.3.2. Transmission electron microscopy (TEM)

The morphological observation of AF nanoparticles was conducted by FEI-Tecnai G2-Spirit transmission electron microscope (FEI, U.S.A.) operating at 120 keV voltage, utilising a tungsten filament. Five microliter of AF was deposited onto a carbon-coated copper grid which is glow discharged by PELCO easy Glow discharge unit. Afterwards, samples were negatively stained with 2% of uranyl acid based on the side blot method. Gatan Ultrascan 4000CCD camera (Gatan, Pleasanton, California, USA) was used for the imaging. Diameters of spherical nanoparticles from 13 different TEM images were quantified by using the ImageJ toolbar.

3.4. Capsaicin content of oleoresins

The capsaicin content of capsicum, chilli birds' eye and chilli ancho oleoresins were analysed by HPLC-UV/VIS (Shimadzu, Columbia, USA), comprising DGU-20 A S degasser, LC-20 AD pump system, SIL-20 A C auto-sampler, CTO-20 A C column oven and UV–Vis (SPD-20 A) detector. Kinetex C18 reversed-phase column (5 μm, 100 Å, 150 × 4.6 mm, 00F-4601-E0; Phenomenex, Torrance, USA) was used for separation. The mobile phases were water (including 0.1% formic acid) and acetonitrile. Capsaicin standard and oleoresin samples were eluted using the gradient shown in Suppl. Table 2 at a flow rate of 1.0 mL/min, 30 °C of column temperature and 20 μL of injection volume. Capsaicin was detected at λ = 280 nm at 11.765 ± 0.024 min after injection and the total runtime of the method was 30 min. Standard and samples were prepared in methanol and seven different concentrations (1, 10, 25, 50, 100, 250 and 500 μg/mL) of capsaicin standard solutions were used for the standard curve ($R^2 = 0.99$). The curve was prepared in real duplicates and samples were created in triplicates.

3.5. Emulsions preparation

Three oleoresin samples of varying source and pungency, namely capsicum, chilli birds' eye, and chilli ancho were used to produce emulsions. Miglyol emulsions (including 1% (v/v) Miglyol) without capsaicin were considered as control emulsions. The capsaicin content of oleoresins can be seen in Table 1.

Capsaicin oleoresin-loaded oil-in-water emulsions were prepared following the workflow shown in Fig. 1. AF was filtered through Whatman filter paper no.3 prior to use in emulsions. Based on a preliminary analysis, the particle size of coarse emulsions was found too high (~3000 nm) to form stable systems and creaming could already be observed on the same day they were prepared. Based on this, we decided to apply two passes of high-pressure homogenisation using a Panda homogeniser (GEA Niro Soavi Homogeniser, Parma, Italy) to these emulsions. This process resulted in the formation of fine emulsions (<644 ± 8 nm), subsequently prototyped and studied.

Table 1
Measured capsaicin content of three different capsaicin oleoresins.

Oleoresin Name	Capsaicin Content (%)
Capsicum	4.14 ± 0.03
Chilli Birds' Eye	2.82 ± 0.03
Chilli Ancho	0.13 ± 0.00

Densities of oil, AF and emulsions (Table 2) were measured by using Anton Paar DMA 4500 M densitometer (Anton Paar GmbH, Austria). Volume fractions (ϕ) (Table 2) were calculated to observe the accuracy of the experiment based on the following formula (Eq. (1)) (McClements, 2005) where ρ_e is the density of the emulsions, ρ_1 is the density of the continuous phase (AF) and ρ_2 is the density of the dispersed phase (oleoresin + Miglyol). The oil volume percentage was obtained from the value of the volume fraction (=$\phi \times 100$).

$$\phi = \frac{\rho_e - \rho_1}{\rho_2 - \rho_1} \quad (1)$$

3.6. Particle size and zeta potential determinations

The particle size distribution, polydispersity index (PDI), zeta potential (ζ) and colloidal stability of AF and chilli oleoresin-in-water emulsions were investigated by scattering and electrophoretic mobility measurements. The particle size was determined by dynamic light scattering (DLS) with non-invasive back scattering (DLS-NIBS) using a Zetasizer Nano ZSU5700 (Malvern Panalytical Ltd., UK) and DTS0012 disposable cuvettes (PMMA, Wertheim, Germany). Measurements were at 25 °C for 30 s with a red laser output (10 mW, λ = 632.8 nm) and a detection angle of 173° backscattered light. The correlograms decay functions were processed by the Zetasizer XPLORER software v.3.2.1 to calculate the hydrodynamic diameter (D_h) from the particle diffusion coefficient (D_p) using the Stokes-Einstein equation (Eq. (2)). Particle size results represent the mean hydrodynamic diameter (D_h) of samples. In this equation, the shape of particles is assumed spherical. K_b and T denote Boltzmann's constant and absolute temperature, respectively, while η is the dynamic viscosity of the fluid (Babick, 2019).

$$D_p = \frac{K_b\, T}{3\,\pi\,\eta\, D_h} \quad (2)$$

To determine the colloidal stability during short-term storage at room temperature (~20 °C), the particle size was monitored for 28 days.

Electrophoretic mobility measurements were performed by laser Doppler velocimetry on the same instrument set-up as for the particle size measurements above operated in the mixed mode measurement phase analysis light scattering (M3-PALS) and using a DTS1070 Zetasizer folded capillary cell (Malvern, UK). The ζ-potential was obtained from the electrophoretic mobility (U_E) using the Henry equation (Eq. (3)) where U_E is the electrophoretic mobility, ε is the dielectric constant, η is the viscosity of the dispersant and $f(Ka)$ is the Henry's function.

$$U_E = \frac{2\,\varepsilon\zeta f(Ka)}{3\,\eta} \quad (3)$$

3.7. Viscosity determinations

The dynamic viscosity of AF and water were measured as average values of three runs at 25 °C using an automated rolling ball microviscometer Lovis 2000 ME module integrated in a DMA Density Meter (Anton Paar, Ostfildern, Germany) described in Section 3.5, with programmable tube angle based on the principle of the rolling ball time (the time that a steel ball needs to roll through the sample inside a calibrated 1.6 mm diameter capillary).

3.8. Statistical analysis

All experiments were conducted in triplicate. Statistical analyses were completed using SPSS Statistics 20, IBM software. One-way analysis of variance (ANOVA) and Tukey comparisons were applied to test any significant differences at a 5% significance level ($p \leq 0.05$).

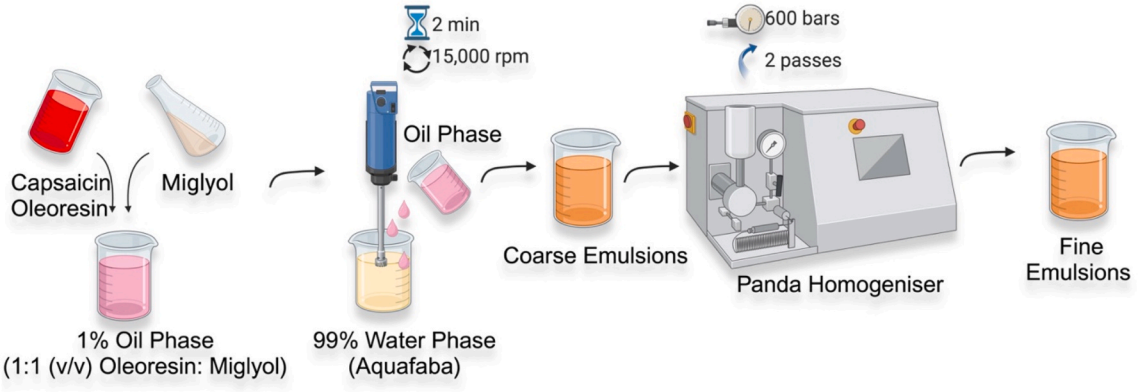

Fig. 1. Production of capsaicin oleoresin-loaded oil-in-water emulsions.

Table 2
Densities (g/cm^3) of oil phase, water phase and emulsions, and the oil phase volume percent (vol.%) in emulsions.

Sample	Density (g/cm^3)	Oil volume percentage (vol. %)
Aquafaba	1.003157 ± 0.000257	–
Miglyol	0.94093 ± 0.000226	–
Miglyol + Capsicum Oleoresin	0.94395 ± 0.000213	–
Miglyol + Chilli Birds' Eye Oleoresin	0.93450 ± 0.000224	–
Miglyol + Chilli Ancho Oleoresin	0.93855 ± 0.000217	–
Control (Miglyol) Emulsion	1.002627 ± 0.000263	0.85 ± 0.015
Capsicum Emulsion	1.002663 ± 0.000293	0.83 ± 0.066
Chilli Birds' Eye Emulsion	1.002593 ± 0.000282	0.82 ± 0.079
Chilli Ancho Emulsion	1.002593 ± 0.000267	0.87 ± 0.052

4. Results and discussion

4.1. Characterisation of British Kabuli Chickpea aquafaba

4.1.1. Dry matter content

The dry matter content of AF was determined as 1.48 ± 0.04%. Previous studies reported up to 3 to 5-fold greater dry matter values. For example, Stantiall, Dale, Calizo, and Serventi (2018) reported a value of 5.13% dry matter in AF from Garbanzo chickpeas (1:1.75 C WR). Recent studies by He, Meda, et al. (2021) observed a dry matter content of 7.6% in AF produced by CDC Leader chickpeas (1:1.75 C WR) and Tufaro and Cappa (2023) found a dry matter of 3.39% in AF from Garbanzo chickpeas (1:1.15 C WR). The lower dry matter content of the AF obtained in our study is attributed to the 5-fold greater CWR used as compared with previous works. In this regard, it could be attributed that a higher water ratio used in this study prevents particle aggregation thus leading to obtaining stable particles of average size <1000 nm. Besides, the phenomena at play governing the migration of soluble (and perhaps insoluble) substances from chickpea seeds to the cooking water are expected to vary depending on the chickpea cultivar, the hull thickness and the cooking conditions (He et al., 2019; Wood, Knights, & Choct, 2011).

4.1.2. Total carbohydrate analysis

The total carbohydrate compositions of the raw and processed chickpea as well as the solid and liquid fractions of AF are as shown in

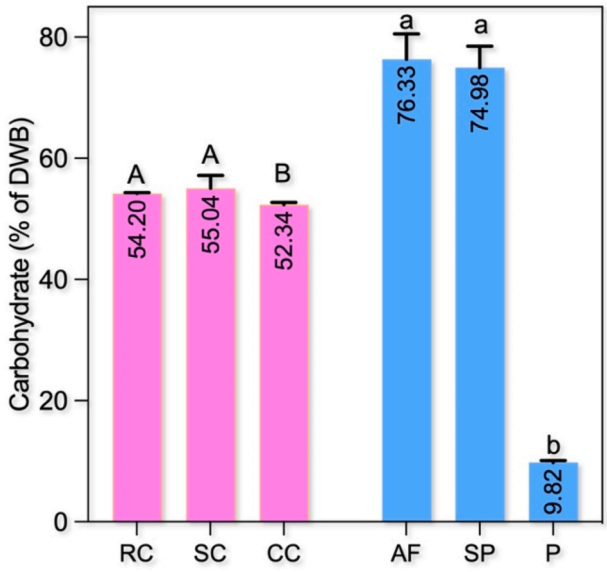

Fig. 2. Total carbohydrate composition of raw chickpea (RC), soaked chickpea (SC), cooked chickpea (CC), Aquafaba (AF), supernatant (SP) and pellet (P). Different capital and lowercase letters denote significant differences for chickpea and AF samples (separated upon centrifugation), respectively ($p \leq 0.05$).

Fig. 2. Of note, the total carbohydrate of chickpeas under the different treatments (raw, soaked and cooked) was found as the primary constituent and changed between 52.34 and 55.85%. These results are in overall agreement with previous studies by de Almeida Costa, da Silva Queiroz-Monici, Reis, and de Oliveira (2006) and Siva, Thavarajah, Kumar, and Thavarajah (2019). Interestingly, the soaking process did not have a significant ($p>0.05$) impact on the carbohydrate composition when comparing the RC versus the SC. By contrast, a significant ($p \leq 0.05$) reduction amounting to ~6% was observed after cooking the SC. This is in keeping with the notion that a fraction of the soluble carbohydrates leach into the cooking water during cooking. These findings are in partial agreement with Xu et al. (2016) who reported no significant ($p > 0.05$) difference in total carbohydrates between RC, SC and CC. On the other hand, Frias, Vidal-Valverde, Sotomayor, Diaz-Pollan, and Urbano (2000) reported that soaking and cooking resulted in a 24% reduction in the available carbohydrate content of the chickpeas. The difference in carbohydrate content observed in this study for cooked chickpeas can be attributed to various factors: i) the structural changes of starch (the major carbohydrate fraction) molecules such as amylose retrogradation, linearisation of amylopectin and starch gelatinisation mostly promoted by temperature, water content and pressure (Siva et al., 2019), ii)

leaching of soluble/insoluble carbohydrate fractions like raffinose, stachyose, sucrose, verbascose and reducing sugars (Alajaji and El-Adawy, 2006).

Further inspection of Fig. 2 shows the variation in total carbohydrate content of AF (76.33 ± 4.20%) as well as its partitioning between the SP and P upon centrifugation. Our data are in overall agreement with the study of He, Meda, et al. (2021) that analysed the carbohydrate content of the dry matter of AF ranging over a wide range of 55–74%. Based on the non-significant difference ($p > 0.05$) between AF and SP results, it can be inferred that AF consists predominantly of water-soluble carbohydrates along with a smaller amount of insoluble carbohydrates that occur in the P. In line with this reasoning, it has been reported that mostly low molecular weight water-soluble carbohydrates such as raffinose, sucrose, and stachyose transfer to the cooking water of chickpeas (Stantiall et al., 2018).

4.1.3. Monosaccharides composition

We gained further insight into the monosaccharides composition of the AF carbohydrates using highly sensitive and selective HPAEC-PAD chromatography, as one of the well-standardised and validated methods for this determination. D-galactose and D-glucose were found as the predominant neutral sugars, followed by L-arabinose and relatively lower proportions of D-xylose and D-fructose (Fig. 3). Siva et al. (2019) reported the presence of glucose, fructose, sucrose, rhamnose, arabinose and xylose in Kabuli type of chickpeas. These monosaccharides or small oligosaccharides that they may comprise (upon hydrolysis by TFA) can easily leach from the seeds to AF while cooking, given their high water solubility. Our results are consistent with the notion that the cooking process modifies the chemical composition of the seeds and presumably reduces the concentration of non-soluble oligosaccharides such as raffinose, sucrose and stachyose as they diffuse into AF (Alajaji & El-Adawy, 2006; Attia, Shehata, Aman, & Hamza, 1994). The presence of galactose can be an indicator of ciceritol di-galactoside which is reported as the main sugar found in chickpeas and some other legumes (lentil and white lupin) (Sánchez-Mata, Peñuela-Teruel, Cámara-Hurtado, Díez-Marqués, & Torija-Isasa, 1998; Xiaoli et al., 2008; Kaur & Prasad, 2021). The monosaccharide composition of pressure-cooked self-prepared AF, as done in this study, has not been documented; however, Shim, Mustafa, Shen, Ratanapariyanuch, and Reaney (2018) also reported glucose and sucrose in the commercially canned AF by using ^{1}H NMR spectroscopy.

Notably, only traces of fructose were detected, thus suggesting that fructose-containing oligosaccharides are relatively minor components of AF, which is in accordance with the results of Tosh et al. (2013) who did not find verbascose in chickpea powder. The absence of verbascose in chickpeas proves that it cannot leach into AF, as these are far less soluble in water. The presence of arabinose and galactose may indicate some dietary fibres like branched pectic polysaccharides, particularly those released from chickpea seed coats. Arabinogalactans consisting of arabinose and galactose monosaccharides are predominantly located on plant cell walls and plasma membranes, forming the core-coat interface of arabinogalactans-proteins (AGP) (Sathyanarayana & Prashanth, 2019). Detection of xylose and arabinose also may be attributed to the presence of hemicellulose which also formed the cell walls released from chickpea hulls (Siva et al., 2019). Glycosidic linkage analysis by NMR or other techniques should be applied in future studies to elucidate in greater detail the source of the monosaccharides obtained. The determined uronic acid contents of samples were as low as 0.1 ± 0.01%, 0.05 ± 0.01% and 0.003 ± 0.00% for AF, SP and P, respectively, thus reflecting a negligible presence of charged polysaccharides such as pectin polygalacturonans or arabinogalactan proteins.

4.1.4. Elemental analysis and protein content

Carbon (C), hydrogen (H) and nitrogen (N) contents of samples were determined by the combustion method and the results can be seen in Table 3. The C% of CC were found similar to previous studies showing 46.20 ± 0.29% carbon of cooked seeds (Shim et al., 2018). CC presented higher C% than RC and SC, while the N%, accordingly protein contents

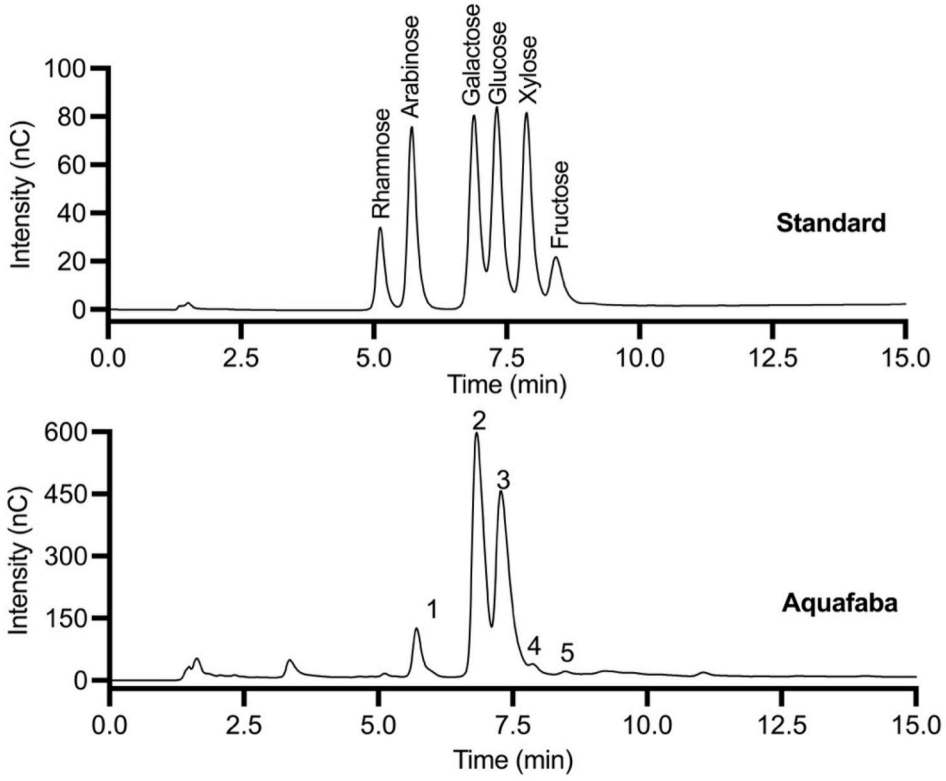

Fig. 3. HPAEC-PAD chromatogram profiles of standard monosaccharide mixture (10 μg/mL) and neutral monosaccharides from AF sample. Peak identity: 1, L-arabinose; 2, D-galactose; 3, D-glucose; 4, D-xylose; 5, D-fructose.

Table 3
Elemental composition and protein content of AF process steps. Data is in DWB.[1].

Sample	Carbon (%)	Hydrogen (%)	Protein (%)[a]
Raw Chickpea	42.44 ± 0.06^{B}	7.11 ± 0.03^{B}	15.04 ± 0.12^{A}
Soaked Chickpea	43.02 ± 0.40^{B}	7.21 ± 0.04^{B}	15.35 ± 0.73^{A}
Cooked Chickpea	45.15 ± 0.50^{A}	7.53 ± 0.08^{A}	15.43 ± 1.23^{A}
Aquafaba	37.24 ± 0.06^{b}	6.57 ± 0.00^{a}	16.29 ± 0.43^{b}
Supernatant	37.02 ± 0.24^{b}	6.51 ± 0.04^{a}	15.92 ± 0.35^{b}
Pellet	41.23 ± 0.60^{a}	6.42 ± 0.03^{b}	26.38 ± 0.64^{a}

[1]Different capital and lowercase letters denote significant differences within each column for chickpea and AF (separated upon centrifugation) samples, respectively ($p \leq 0.05$).

[a] Protein content is estimated as total nitrogen (N) content multiplied by 6.25.

remained unchanged ($p > 0.05$). This causes an increase in the C: N ratio from RC to CC, which can be explained by the swelling of available starch and its subsequent leach of amylose or amylopectin with the effect of heat and water during cooking (Aguilera, Esteban, Benítez, Mollá, & Martín-Cabrejas, 2009). In general, the protein content of British Kabuli chickpeas was found to be lower than in previous studies, such as 22% (Erem et al., 2021) and 25.1% (Xu et al., 2016).

The C% of AF was consistent with Shim et al. (2018), although the protein content (16.29 ± 0.43%) was lower compared to their observation of canned AF, which ranged between 22.65 and 26.83%. On the other hand, Cabrita et al. (2023) and Raikos et al. (2020b) reported the protein content of commercial powdered AF as 19% and 17.8%–19.6%, respectively, which aligns closely with our findings. The protein phenomena in our study can be attributed to the comparatively low protein level of chickpea seeds compared to some previous studies, resulting in a limited transfer to the cooking water. Additionally, harvest-related, climatic, cultivar reasons, process conditions such as temperature, cooking water ratio (CWR), and preservatives added to canned chickpeas can influence the compositional properties of AF (Erem et al., 2021). The high protein % observed in the P can be attributed to the relatively higher dry matter content within the P. It appears that the insoluble proteins that remain in the P after centrifugation contribute to higher dry matter and overall, a higher protein concentration (Han, Swanson, & Baik, 2007).

4.1.5. SDS-PAGE analysis

The electrophoresis gels of RC, SC and CC revealed a wide range of protein profiles between ~2 up to ~98 kDa, while AF and SP showed a range between ~2 up to ~80 kDa with a notable prevalence of low MW proteins (~2–16 kDa) (Fig. 4). Chickpea samples displayed a detected band with high MW at ~98 kDa (A) which can be assigned to the lipoxygenase, in agreement with previous studies (Buhl, Christensen, & Hammershøj, 2019; Chang, Alli, Konishi, & Ziomek, 2011; Deep Singh, Wani, Kaur, & Sogi, 2008); convicilin/vicilin precursors at 70 kDa (C) (Bar-El Dadon et al., 2013; Grasso et al., 2022); and 11 S legumin at 39 kDa in non-reducing conditions (E) (Alsalman & Ramaswamy, 2021). In contrast, AF samples revealed a decreased intensity on the CC's protein bands (lines 3) due to the effect of cooking on changes in protein secondary structure (Xu et al., 2017).

The band at ~80 kDa (B) detected in all samples in both reducing and non-reducing conditions was reported as unspecified in Crawford, Tyl, and Kerr (2023), however, named as 'albumin fractions' in Papalamprou, Doxastakis, Biliaderis, and Kiosseoglou (2009). Provicilin/vicilin precursors at the 50 kDa band (D) were intensely detected in chickpea samples, however, this was also slightly detected in AF samples (Raikos et al., 2020b). Based on previous studies the bands may indicate acidic subunit 11 S legumin at 35 kDa (F) and 20 kDa (H) (Crawford, Tyl, & Kerr, 2023); albumin fractions at 31 kDa (G) (Papalamprou et al., 2009); γ-subunit of 7 S vicilin at 16 kDa (I) (Buhl et al., 2019; Crawford, Tyl, & Kerr, 2023); histone proteins at 14.8 kDa (J) (Alsalman & Ramaswamy, 2021; Shim et al., 2018); 2 S albumin at 12 kDa (K) (Alsalman & Ramaswamy, 2021; Crawford, Tyl, & Kerr, 2023); and defensin at 8 kDa (L) (Raikos et al., 2020b; Shim et al., 2018). The band located at 2.2 kDa (M) can be attributed to the low-MW chickpea peptides which are cicerin (2.2 kDa) (UniProtKB, 2004b) and arietin (1.9 kDa) (UniProtKB, 2004a).

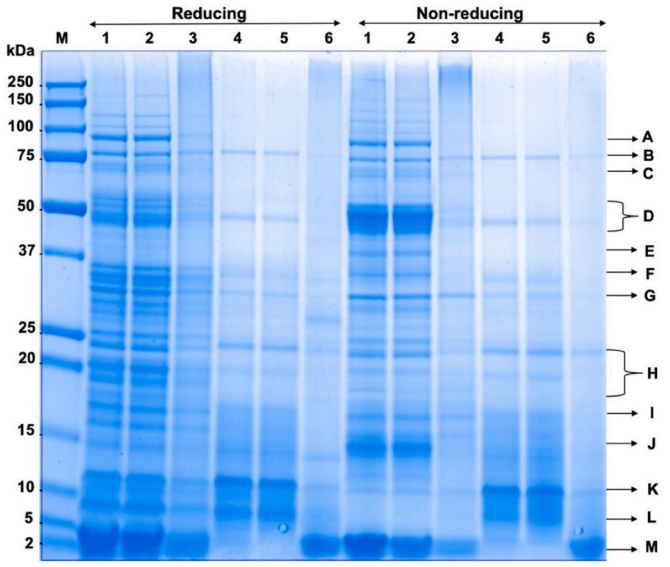

Fig. 4. SDS-PAGE analysis of raw chickpea (RC) (lanes 1), soaked chickpea (SC) (lanes 2), cooked chickpea (CC) (lanes 3), aquafaba (AF) (lanes 4), supernatant (SP) (lanes 5) and pellet (P) (lanes 6) under both reducing and non-reducing conditions. Lane M: MW standards (kDa). Protein band: (A) 98 kDa: lipoxygenase; (B) 80 kDa: albumin fractions; (C) 70 kDa: convicilin/vicilin precursors; (D) 50 kDa: provicilin/7 S vicilin precursors; (E) 39 kDa: 11 S legumin; (F) 35 kDa: acidic subunit 11 S legumin; (G) 31 kDa: albumin fractions; (H) 20 kDa: 11 S legumin; (I) 16 kDa: γ-subunit of 7 S vicilin; (J) 14.8 kDa: histone proteins; (K) 12 kDa: 2 S albumin; (L) 8 kDa: defensin; (M) 2.2 kDa: cicerin/arietin.

Of note, it seems clear that low MW proteins (≤~16 kDa) transfer to the AF from RC in agreement with previous studies (Buhl et al., 2019) that reported proteins of MW ≤ ~24 kDa. Therefore, we argue that AF proteins consist of mostly water-soluble albumins and globulins which remain in the SP (lines 5), while some insoluble proteins (possibly glutelins and prolamins representing a small fraction of total proteins in chickpea) and potential peptides remain in the P (lines 6). Due to the effect of DTT reduction, bands were observed at around 50 kDa, 15 kDa and 12 kDa these appeared as a result of disulfide bond breakdown, which is also reported by Lin et al. (2020).

4.1.6. Saponins content

Saponins content of raw British Kabuli chickpea (RC) was 17.57 ± 0.52 mg/g. Kaur, Kaur, Gupta, and Kaur (2016) observed varied saponins content between 15.30 and 40.92 mg/g from 18 different chickpea cultivars and Ercan and El (2016) reported 24.1 mg/g, which illustrates the saponins content is predominantly affected by varietal effects and growing conditions such as climate, soil alkalinity/acidity, excess/lack of water, etc. No significant difference in saponins content was observed by the soaking process ($p > 0.05$), in contrast to the same study which found a 44.94 % reduction in the saponins content of chickpeas after 24 h soaking (Kaur et al., 2016). On the other hand, Ruiz et al. (1996) found no significant impact of soaking on the saponins content of chickpeas. During cooking, 45.36% of saponins was lost (Fig. 5) which is consistent with Srivastava and Vasishtha (2013) who detected a substantial decrease (66.3%), and with Erem et al. (2021) who reported a 40% reduction in the overall saponins level and the transfer of the rest of the saponins to the AF based on the water-soluble nature of saponins (Sánchez-Velázquez et al., 2021). The reason for the mitigation of

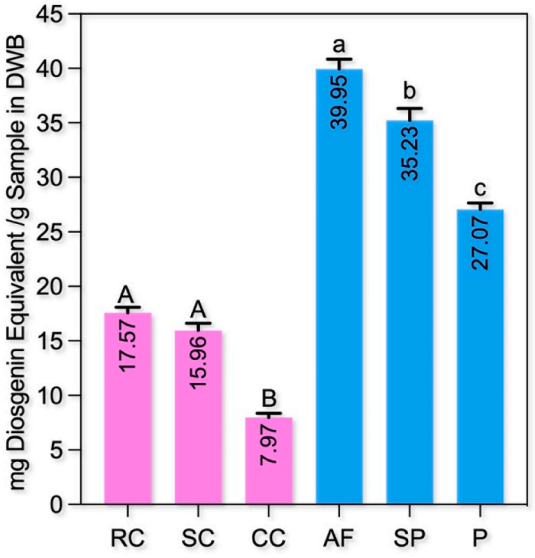

Fig. 5. Saponins content of raw chickpea (RC), soaked chickpea (SC), cooked chickpea (CC), Aquafaba (AF), supernatant (SP) and pellet (P). Different capital and lowercase letters denote significant differences for chickpea and AF samples (separated upon centrifugation), respectively ($p \leq 0.05$).

saponins is that, under pressure and temperature conditions, the linkage bonds between the oligosaccharide moieties and saponin molecules break down, therefore saponins leak from seed coats to the cooking water (Yu, Patterson, & Zaharia, 2022). Moreover, possible enzymatic and chemical degradations of saponins during cooking may also account for this observation (Singh, Singh, Singh, & Kaur, 2017).

A high amount of saponins transferred from RC to AF, amounting to 39.95 ± 0.89 mg/g saponins content in DWB. Stantiall et al. (2018) produced AF from Garbanzo chickpeas and reported 4.5 mg/g (DWB) of saponins. On the other hand, Mustafa and Reaney (2020) have reported a wide range of saponins content for AF from 4 to 30 mg/g. Since saponins are secondary metabolites which can be affected by pulse species, the ecological and agronomic conditions during plant growth, genetic origin and post-harvest treatments, the content can vary among different AF samples obtained from different chickpeas (Güçlü-Üstündağ & Mazza, 2007). On the other hand, saponins content in AF may present a higher extraction rate compared to chickpeas due to the two-step extraction, first aqueous extraction during cooking and subsequent extraction with 80% methanol, thus, potentially increasing the saponins content in AF, SP and P.

Furthermore, a significant difference ($p \leq 0.05$) was observed between AF and the SP obtained after centrifugation. In the pellet, 27.06 ± 0.58 mg/g of saponins were found to remain, as these can form complexes with proteins at low pH and/or during heating processing (Morton & Murray, 2001; Potter, Jimenez-Flores, Pollack, Lone, & Berber-Jimenez, 1993). Moreover, this phenomenon might be explained by the hydrophobic interaction of amphiphilic saponin molecules and hydrophobic components that are partitioned in the pellets such as lipids, insoluble fibres, and hydrophobic proteins, thus resulting in the precipitation of saponins. Moreover, the interaction of saponins with proteins and oligosaccharides or adsorption onto solid surfaces can lead to their adherence and decreased solubility in water (Li, Liu, Liu, & Zhu, 2022).

4.1.7. Total phenolics content

The impact of employing different methods (Folin-Ciocalteu and Fast Blue BB) and solid phase extraction to eliminate polar interferences have been studied on RC, SC, CC, AF, SP and P (Table 4). While solid phase extraction prior to the Folin-Ciocalteu reaction did not change ($p > 0.05$) the phenolic content in all samples; removal of interferences in all except the CC sample was observed ($p \leq 0.05$) before the Fast Blue BB assay. This phenomenon shows that possible interferences such as reducing sugars, proteins, monosaccharides, and aromatic amino acids tyrosine which are present in chickpeas (Pico et al., 2020) can cause an overestimation of total phenolics content, thus it is necessary to add a clean-up step by SPE. Moreover, it is observed that the Fast Blue BB reaction was more effective for quantifying total phenolics coupled with the removal of the interferences present in the phenolic extracts than the Folin-Ciocalteu method. The specific reaction between the diazonium group of Fast Blue BB and the aromatic ring by activating hydroxyl groups (-OH) eliminates the possible Fast Blue BB-interferences interaction and increases the sensitivity for phenolics (Pico et al., 2020). RC presented a total phenolics content of 1.21 ± 0.12 mg/g (from EPP) and 1.34 ± 0.00 mg/g (after SPE) ($p > 0.05$), measured by the Folin-Ciocalteu method. Pico et al. (2020) and Campos-Vega, Loarca-Piña, and Oomah (2010) reported a total phenolics content in chickpeas of 0.88 mg/g and 1.81 mg/g, respectively by using the same method.

Table 4
Extractable phenolic compounds (EPP) measured without interferences removal (control) and after removal of interferences by solid phase extraction (SPE) of RC, SC, CC, AF, SP and P by Folin-Ciocalteu and Fast Blue BB reactions.

Sample	Folin-Ciocalteu		Fast Blue BB	
	Control (mg/g)	SPE (mg/g)	Control (mg/g)	SPE (mg/g)
Raw Chickpea[1]	1.21 ± 0.12^{Ab}	1.34 ± 0.00^{Ab}	2.14 ± 0.30^{Aa}	1.19 ± 0.04^{Ab}
Soaked Chickpea[1]	1.14 ± 0.15^{Ab}	1.27 ± 0.10^{Ab}	2.48 ± 0.01^{Aa}	1.25 ± 0.19^{Ab}
Cooked Chickpea[1]	0.79 ± 0.05^{Bc}	0.88 ± 0.03^{Bbc}	1.10 ± 0.02^{Ba}	0.97 ± 0.01^{Aab}
Aquafaba[2]	7.05 ± 0.03^{Ab}	7.22 ± 0.33^{Ab}	8.77 ± 0.09^{Aa}	7.48 ± 0.17^{Ab}
Supernatant[2]	6.80 ± 0.09^{Abc}	7.18 ± 0.36^{Aab}	7.88 ± 0.12^{Ba}	6.24 ± 0.27^{Bc}
Pellet[2]	4.46 ± 0.15^{Bc}	4.98 ± 0.14^{Bc}	7.99 ± 0.26^{Ba}	6.33 ± 0.10^{Bb}

[1]Different capital letters represent the significant differences ($p \leq 0.05$) within each column and different lowercase letters represent the significant differences ($p \leq 0.05$) within each row for only chickpea samples.
[2]Different capital letters represent the significant differences ($p \leq 0.05$) within each column and different lowercase letters represent the significant differences ($p \leq 0.05$) within each row for only aquafaba samples (separated upon centrifugation.

After soaking there was no significant difference ($p > 0.05$), however, by cooking remarkable reduction was observed with all methods ($p \leq 0.05$) on phenolics. This can be explained by the heat-sensitive properties of phenolics whose degradation can be triggered by heat exposure and enzymatic reactions (Nicoli, Anese, & Parpinel, 1999), while no heat application prevents the degradation of phenolics in the soaking process. Another explanation of this thermal degradation can be the oxidation of hydroxyls since most phenolic compounds are non-conjugated which leads to the degradation of these functional structures (Vallverdú-Queralt, Regueiro, Rinaldi de Alvarenga, Torrado, & Lamuela-Raventos, 2014).

AF, SP and P also demonstrated the same approach regarding the application of Folin-Ciocalteu and Fast Blue BB methods before and after SPE (Fig. 6). Freeze-dried AF presented 7.05 ± 0.03 mg/g total phenolics content by Folin-Ciocalteu assay which showed no significant difference ($p > 0.05$) after SPE (7.22 ± 0.33 mg/g). However, a significant reduction ($p \leq 0.05$) was observed in the Fast Blue BB between EPP (8.77 ± 0.09 mg/g) and SPE (7.48 ± 0.17 mg/g). Although the removal of interferences was successful in Fast Blue BB, total phenolics content within AF showed similar results in both techniques. Raikos et al. (2020a) reported similar results by the application of Folin-Ciocalteu on dried AF and found 6.50 ± 0.00 mg/g total phenolics expressed as gallic

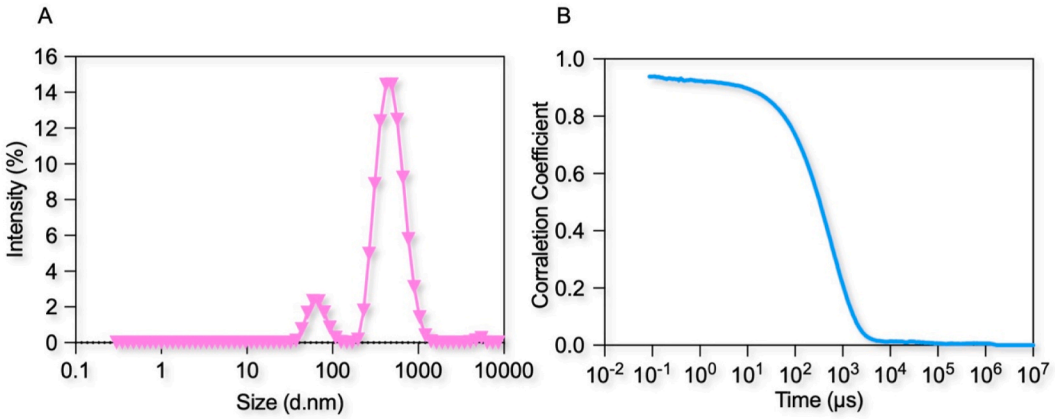

Fig. 6. Representative plots of particle size intensity distribution (A) corresponding correlogram (B) to estimate the hydrodynamic diameter (D_h) distribution of AF obtained from British Kabuli chickpea. Measurements were done after filtration of AF through Whatman filter paper no.3.

acid/g of dried AF. Additionally, the seed composition, cultivar and degradation due to the various processing conditions can impact the content of secondary metabolites like phenolics (Shim et al., 2018).

4.2. Incidental aquafaba nanoparticles

Boiling chickpeas in water promotes structural and conformational changes in the comprising protein and polysaccharide components via covalent bonds and non-covalent interactions. For example, the Maillard reaction results in the covalent links between proteins and polysaccharides (Mustafa & Reaney, 2020). Moreover, phenolics and saponins found in AF could facilitate the formation of protein-polysaccharide complexes via hydrogen bonding and hydrophobic interactions (Buhl et al., 2019). Based on these phenomena, we investigated the formation of colloidal complexes (micro and nanoparticles) by probing the particle size distribution and zeta potential of AF.

The colloidal particles exhibited a bimodal size distribution comprised of particles of <~100 nm and <~1000 nm as shown in Fig. 6A. Typically, hydrodynamic diameter (D_h) is determined by measuring the mean diameter depending on intensity using dynamic light scattering (DLS). Although the proportion of larger particles dominates the intensity distribution measured by DLS (Ryan et al., 2012), Fig. 6A shows the existence of the smaller nanoparticles. The Z-average D_h of the two peaks was approximately ~59 nm and ~489 nm, respectively. Moreover, the homogeneity of AF systems and the quality of measurements can also be seen from the correlogram (Fig. 6B).

The presence of nanoparticles (D_h < ~100 nm) in AF is consistent with the notion that Pickering emulsions can be formed by AF. In line with this idea, Ren, Chen, Zhang, Lin, and Li (2019) (tea water-insoluble protein nanoparticles between 30-200 nm and 200–1000 nm) and Xiao, Wang, Gonzalez, and Huang (2016) (kafirin nanoparticles with two size regions which were ~90 nm and ~340 nm) observed the two distribution peaks from potential food-grade Pickering particles and obtained well-qualified stable systems. The formation and stability of oil-in-water emulsions of AF are addressed in the following section.

The stability of AF nanoparticles upon refrigeration (4 °C) storage was investigated. The D_h of AF was 612 ± 16 nm on day 0, and this value increased to 792 ± 38 nm on day 7 ($p \leq 0.05$), beyond which the particle size remained approximately constant ($p>0.05$) for 28 days of storage and AF medium continued to contain small particle size distribution throughout the storage period. Based on this evidence, we argue that particles maintained their colloidal stability even though their average size increased mildly in the first week of storage, as supported by the constant PDI values below 0.5 (Fig. 7) and steady ζ-potential value ($p > 0.05$) which was −22.3 ± 0.4 mV throughout the storage (Fig. 7). Ke et al. (2015) also studied self-assembled protein-aconitine nanoparticles in the boiling water extracts of licorice roots, which showed D_h ranging from 100 to 500 nm. Moreover, the study revealed notable effectiveness in terms of the stability and capabilities for encapsulation of these nanoparticles (Ke et al., 2015).

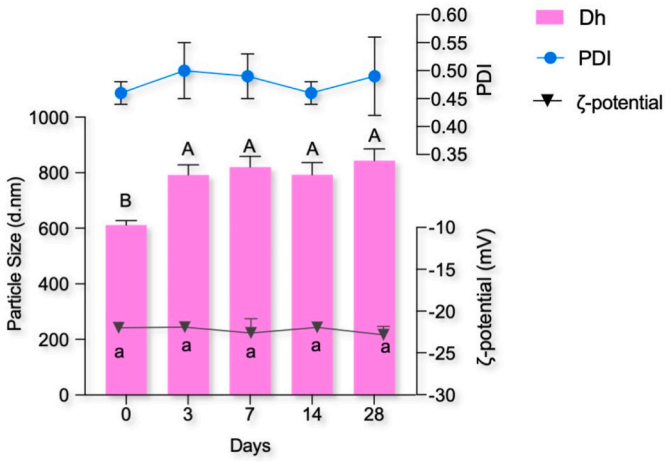

Fig. 7. Evolution of the particle size (hydrodynamic diameter, D_h), PDI and ζ-potential of AF over time at 4 °C. Measurements were done after filtration of AF through Whatman filter paper no.3. Different capital and lowercase letters denote significant differences for particle size and ζ-potential values respectively ($p \leq 0.05$).

Additional characterisation of the size and morphology of AF nanoparticles was performed through TEM visualisation (Fig. 8). From Fig. 8A, the overall population of nanoparticles and the existence of possible macromolecule chains in AF which would participate in the formation of chilli oleoresin-in-water Pickering emulsion can be seen. In general, AF nanoparticles consist of both spherical and non-spherical shapes. TEM images corroborate the findings from DLS, demonstrating the presence of a mixture of particles with sizes of <~100 nm. Quantification of the nanoparticles ($n = 58$) diameters with varying sizes (from $D_{min} = 12.5 \pm 0.6$ to $D_{max} = 71.4 \pm 1.5$ nm), obtained from 13 different TEM images, revealed an average diameter (D_{mean}) of 28.4 ± 12.2 nm.

Although similarities with the small particle size distribution nanoparticles measured by DLS ($D_h = 59$ nm) are encountered in the TEM results such as $D_{mean} = 71.4 \pm 1.5$ nm (Figs. 8C) and 60.8 ± 1.5 nm (data not shown) the average particle size measured in TEM ($D_{mean} = 28.4 \pm 12.2$ nm) was somewhat generally smaller than that obtained by DLS

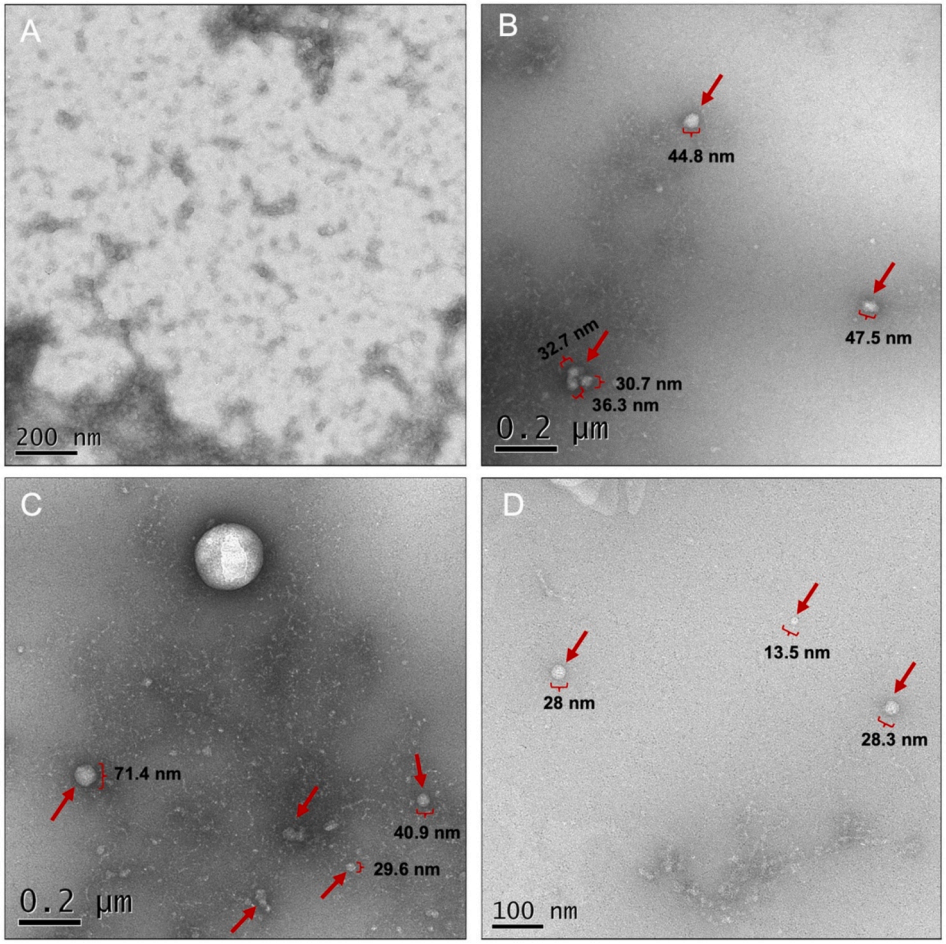

Fig. 8. Negative stain transmission electron micrographs (TEM) of aquafaba (filtered through Whatman filter paper no.3) nanoparticles (A; undiluted, B, C, D; 1:10 diluted sample). Magnifications are shown in bars. Particles were shown with arrows.

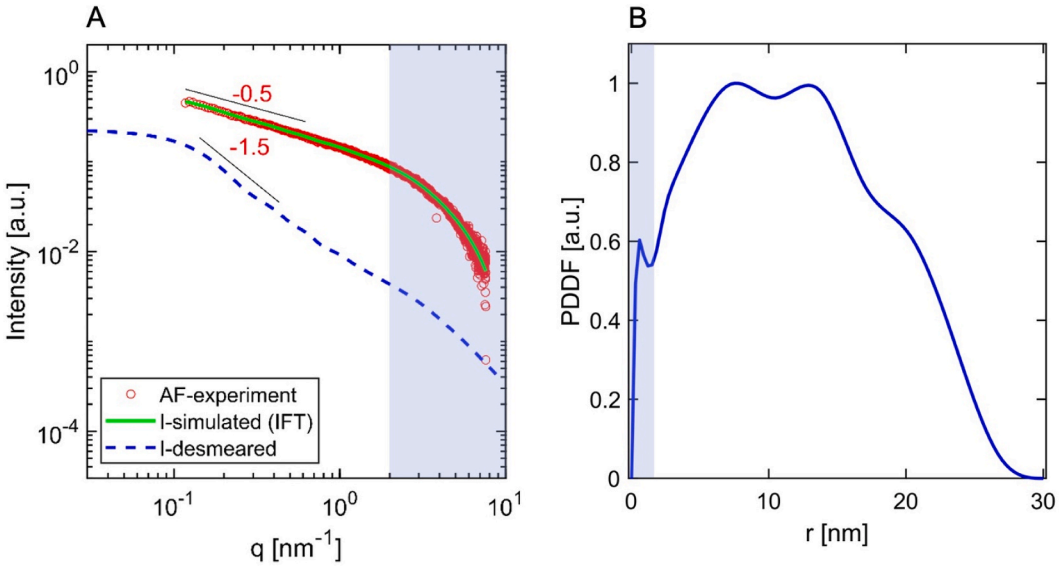

Fig. 9. (A) SAXS profile of polysaccharide-protein complex structure from filtered (Whatman filter paper no.3) AF. Red circles show the experimental data and the solid line represents the simulated profile calculated by indirect Fourier transformation (IFT) analysis, assuming arbitrary-shaped particles are present in the sample. (B) The Pair-Distance Distribution Function (PDDF) of the nanoparticles with respect to the radial distance r (nm). The shaded area in both curves highlights the real-space dimensions below 2 nm. The theoretical desmeared curve (dash line) is extrapolated for $q < 0.1$ taking into account $D_{max} = 30$ nm.

($D_h = \sim$59 nm). A similar phenomenon was also observed in the study by Lin et al. (2020) with the smaller protein nanoparticle size observation in TEM imaging compared to particle size data obtained by DLS. This can be attributed to the higher degree of hydration of the particles and extension of the hydrophilic groups attached to the complex in an aqueous environment (DLS) than in a dry environment (TEM).

SAXS was used to investigate further aspects of the structure of filtered AF samples. The SAXS profile (Fig. 9A) shows a monotonic decay in scattering intensity throughout a broad q range from around 0.1 nm^{-1} to 2 nm^{-1}. The scattering follows a power law in a double logarithmic graph with an apparent slope of $-\frac{1}{2}$ (i.e., the scattering intensity, $I(q)$, is proportional to $q^{-1/2}$. However, it is noteworthy that this scattering profile has been recorded in a SAXSpace camera with line collimation (*i.e.*, a rectangular-shaped X-ray beam with 20 mm length and 0.5 mm width). As a result, the scattering intensities are smeared (convoluted) and the apparent power-law does not represent its actual value. Hence, desemearing is required prior to the interpretation of decay rates in the scattering profile. To correct for the instrumental effect and obtain the actual scattering intensities, the desmeared profile is calculated using the scattering beam length profile and applying an iterative method that has been described and established by Lake (1967). In Fig. 9A, the slit-corrected scattering profile has been presented by a dash-line (the curve is vertically shifted for better clarity). The desmeared curve demonstrates a power law of −1.5 (*i.e.*, the scattering intensity is proportional to $q^{-3/2}$). This decay rate can be associated with scattering from swollen chains of unfolded proteins in the aqueous environment (Beaucage, 1996). Beyond 2 nm^{-1}, (the highlighted region) a much faster decay of scattering intensity has been observed that could be attributed to small-scale (1–2 nm) domains of high electron density.

Nevertheless, our independent investigation of AF dispersion by DLS, TEM and zeta potential measurements all concur with the notion that polysaccharide/protein complex nanoparticles are formed in the range of a few tens of nanometers, showing relatively high colloidal stability. Based on this primary knowledge, the SAXS profiles were interpreted as intensities originating from arbitrarily shaped 3D nanoparticles. Hence, we applied the model-free IFT (Indirect Fourier Transformation) calculation to approximate the size and shape of potential nanoparticles. As a result, the scattering curve from the filtered AF sample was simulated, and a pair-distance distribution function (PDDF) was acquired. The PDDF demonstrates a small peak within the 2 nm range (the highlighted region in small distances in Fig. 9B) and a broad prominent peak. The broad peak shows an asymmetric shape with a peak height of around 10 nm, tailing towards the maximum dimension at 30 nm. Such asymmetric shape PDDF can be attributed to either the polydisperse nanoparticle system (Sadeghpour, Pirolt, & Glatter, 2013) or the elongated ellipsoid-like particles (Glatter, 2018). Irrespective of how we describe the asymmetry of the prominent peak in PDDF, the analysis provides an average gyration radius (R_g) of 9.6 ± 0.1 nm for the potential nanoparticles in this system.

Nanoparticles with ~10 and ~20 nm diameter were also detected in the TEM images (Fig. 8D). This suggests that while there may be some differences, the TEM visualisation (D_{mean} = 28.4 ± 12.2 nm) broadly exhibits close results with the maximal dimension observed by SAXS, both pointing to the presence of small nanoparticles. However, the SAXS diameter ($=2\cdot R_g$) and the mean diameter measured by TEM were smaller than the data ($D_h = \sim$59 nm) obtained from DLS measurements. The difference between SAXS and DLS results may arise from the inherent methodological verities, which can lead to distinct interpretations of particle sizes, also reported by Aengenheister et al. (2018). Moreover, greater values obtained from hydrodynamic radius (R_h) than gyration radius (R_g) were also reported by Kiselev et al. (2013) and explained by the fact that R_g is a static technique derived from X-ray contrast, whereas R_h is a dynamic measurement determined in a solution based on the diffusive motion of the particles, which includes both particles and their associated hydration water. Additionally, depending on the setup resolution, SAXS is limited to detect particle sizes up to approximately 100 nm, while DLS serves as a complementary method to reveal larger particles (Aengenheister et al., 2018). We note that the resolution of our X-ray scattering setup dictates applying the maximum dimension (D_{max}) of 30 nm, and hence, a plateau has been estimated in the theoretical dashed curve at $q < 0.1$ nm^{-1} (see Fig. 9A). Nevertheless, the presence of bigger polysaccharide/protein complexes cannot be excluded, as it goes beyond our SAXS data resolution. Besides, DLS employs the dynamic viscosity of water, which is measured as 0.897 ± 0.05 mPa s, while the measured dynamic viscosity of AF was 1.3466 ± 0.066 mPa s at 25 °C. According to the Stokes-Einstein equation (Eq. (2)), utilising a lower dynamic viscosity in DLS calculations results in an overestimation of hydrodynamic diameter (D_h). This explains the larger particle sizes observed in the DLS results compared to SAXS and TEM, attributing the disparity to the viscosity-based calculations.

4.3. Granular properties and physical stability of AF-capsaicin oleoresin emulsions

Firstly, the influences of high-pressure homogenisation on the particle size of AF in aqueous suspension were addressed at the same homogenisation conditions as for the capsaicin oleoresin emulsions. The D_h of homogenised AF was 277 ± 15 nm and PDI was 0.397 ± 0.06, illustrating the high-pressure homogenisation significantly reduced AF particles' size. The Z-average D_h of emulsions throughout the 28 days of storage is shown in Fig. 10. The particle size of the control emulsion which includes only Miglyol as an oily phase was 245 ± 1 nm on day 0, slightly increased ($p \leq 0.05$) to 266 ± 5 nm on day 3 and reached 276 ± 5 nm on day 7 ($p \leq 0.05$). Afterwards, the system stayed stable through the rest 21 days ($p > 0.05$). Capsicum emulsion was the closest to the control emulsion regarding particle size. While the zero-day showed 283 ± 4 nm, the size increased to 309 ± 2 nm and no significant change ($p > 0.05$) was observed in particle size for the following days. On the other hand, emulsions prepared with chilli birds' oleoresin (2.82% capsaicin content) showed lower stability than capsicum oleoresin (4.14% capsaicin content) and control emulsion by increasing the particle size after 3rd (403 ± 4 nm) and 14th day (426 ± 29 nm) significantly ($p \leq 0.05$). The chilli ancho oleoresin (0.13% capsaicin content) emulsions exhibited the least stability and quick creaming was observed, as indicated by the particle size increase from 644 ± 8 nm initially to 689 ± 4 nm after 28 days.

When emulsions were compared among themselves at the same storage period, all including the control emulsions showed statistically significant differences ($p \leq 0.05$) from each other, thus demonstrating a considerable effect of oil phase type on emulsion particles. Considering the general approach of emulsions, the most stable emulsion was capsicum with both their proximity to control samples and minimal fluctuations in particle size. Conversely, chilli ancho emulsions showed the lowest stability with pronounced increases and alterations of particle size. While capsaicin content (%) of oleoresins shows a descending trend following the order of capsicum (4.12%), chilli birds' eye (2.82%) and chilli ancho (0.13%) order (Table 1), the particle size of emulsions tended to grow in the same order which triggered the instability. The same trend was observed in the study of Wu et al. (2022) who prepared capsaicin emulsions stabilised by sodium alginate and they found that the higher content of capsaicin decreased the droplet size of emulsions. This correlation might be elucidated by different aspects: i) the potential interactions between AF nanoparticles and capsaicin, leading to the formation of complexes that reduce the interfacial tension between oil-water phases (Wu et al., 2022), ii) the high lipophilicity of capsaicin, which results in its superior solubility in the oil (Kim et al., 2014). Capsicum emulsions can have higher stability based on the well-interaction between capsaicin-Miglyol, a more homogenous and stable organic phase can be obtained. On the contrary, in chilli ancho emulsion, including the lowest capsaicin content, other compounds in oleoresin can have less lipophilic properties which limit the

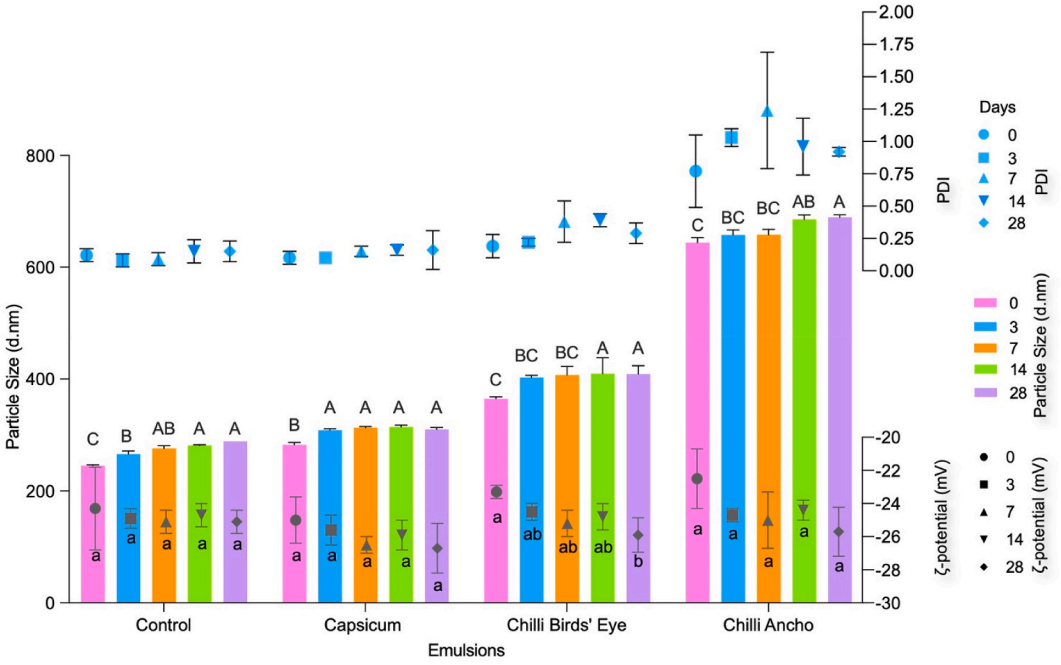

Fig. 10. Evolution of the particle size measurements and PDI of capsaicin oleoresin-loaded emulsions stabilised with AF. Different capital and lowercase letters denote significant differences in particle size and ζ-potential values respectively ($p \leq 0.05$).

solubilisation of oleoresin in Miglyol**.** Consequently, these insoluble structures can easily separate from the oily phase over time, leading to emulsion instability.

The polydispersity index (PDI) of emulsions is also an indicator of their homogeneity and stability. PDI of control and capsicum emulsions always showed ≤0.2 value (Fig. 10) which is considered indicative of the system having a narrow size distribution and adequate stability (Babick, 2019; J. Han, Zhang, Liu, & Xiao, 2020). The PDI of chilli birds' emulsions reached the maximum value on day 14 (0.38 ± 0.05), supporting the initiation of instability. The most fluctuating and high values in PDI data were seen in chilli ancho emulsion. While the PDI of this emulsion on day 0 was 0.77 ± 0.28; it reached 1.25 ± 0.24 on day 7 and after that decreased to 0.92 ± 0.03 on day 28. This change can be explained by the significant ($p \leq 0.05$) increase in particle size from the 7^{th} day onwards, while the decrease in PDI towards 28 days is attributed to the enlargement and aggregation of the majority of the particles. Therefore, the system starts to exhibit a narrow size distribution with enlarged particles. ζ-Potential values of emulsions remained fairly constant ($p > 0.05$) within all emulsions, as shown by the appearance of the various formulations (Fig. 10). The mean ζ-potential of 28 days for capsicum emulsions was −26.1 ± 0.4 mV, which is considered a stable system (Sukhotu et al., 2016). These findings can support the hypotheses proposing that capsicum oleoresin:Miglyol molecules were coated on the surface of AF nanoparticles thereby facilitating the formation of Pickering systems (Su et al., 2020). Chilli ancho emulsions showed a slightly higher value (−24.6 ± 0.4 mV) than capsicum emulsions. However, it still did not show any significant change during storage ($p > 0.05$) although the droplets exhibited a tendency to aggregate in this

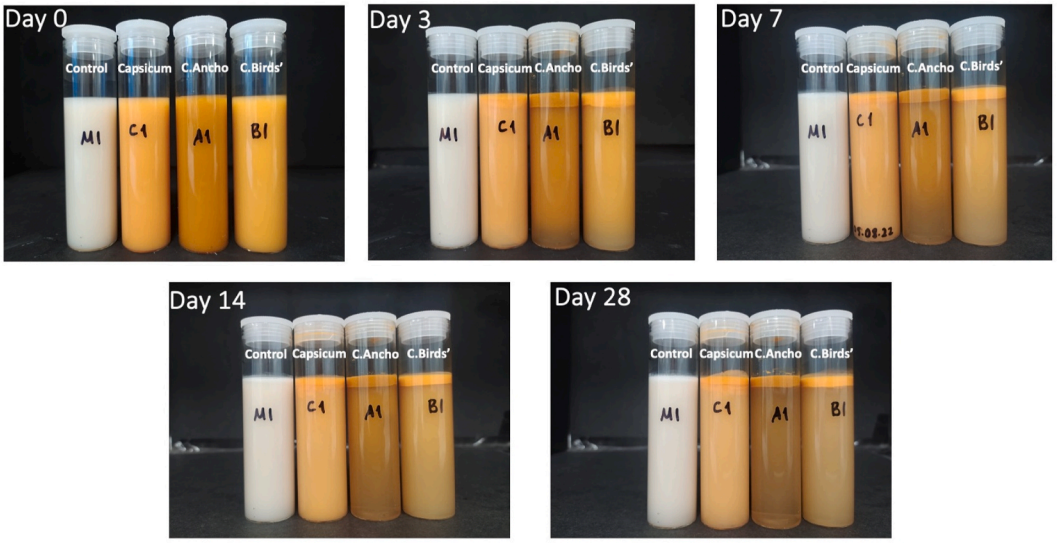

Fig. 11. Physical appearance of emulsions during 28 days of storage. (M1: control (Miglyol) emulsions, C1: capsicum emulsions, A1: chilli ancho emulsions and B1: chilli birds' eye emulsions).

period. This implies that the electrostatic interactions were not the only considerable colloidal interactions to provide overall stability against particle aggregation. The protein-polysaccharide complexes can potentially induce longer-range steric repulsion between particles, thereby enhancing the aggregation stability of droplets (Gumus, Decker, & McClements, 2017).

During the storage period, 'creaming', a reversible instability mechanism, was observed in emulsions (Fig. 11). While this gravitational separation started from day 3 in chilli ancho and chilli birds' eye oleoresin emulsions, it was slightly observed from day 28 onwards in capsicum and control emulsions. Visual inspection of emulsions supports the stability of capsicum emulsions, attributed to the reduction in the particle size distribution, which prevents creaming by allowing globules to remain suspended due to Brownian motion (Krog, 2011). In contrast, instability was obvious in the case of chilli ancho emulsions. A similar instability phenomenon was reported in a study investigating the Pickering capabilities of incidental nanoparticles derived from protein isolate (perilla). In the same study, after 7 days, creaming was seen in some emulsions and this situation was attributed to the reversible adsorption of nanoparticles at the oil-water interface (Zhao, Wang, Hong, Liu, & Li, 2021).

5. Conclusion

In summary, AF produced from the British Kabuli chickpeas was examined and some compositional differences were observed compared to the previously reported results attributed to the variety of chickpeas used and the characteristics of the applied processing methods. The potential formation of AF nanoparticle complexes was investigated, and their emergence during the cooking process of chickpeas was observed. The AF nanoparticles were primarily formed by polysaccharide-protein complexes supported by the presence of saponin and phenolic compounds, as evidenced by DLS, TEM and SAXS measurements, although SAXS, on its own, does not exclude the scattering from swollen chains formed by unfolded protein in the good solvent. To evaluate the contribution of these nanoparticles to the Pickering emulsion formation, capsaicin oleoresin-loaded emulsions were prepared, and they remained stable generally throughout 28 days of storage although their stability levels were diverse based on the oleoresin type. Of note, capsicum oleoresin emulsion, with the highest capsaicin content, showed the best storage stability compared to both birds' eye and ancho chilli oleoresins emulsions. Advanced comparative studies using different techniques like asymmetric-flow field flow fractionation (AF4) will further support the contribution of AF nanoparticles and the presence of unfolded protein chains established in our study towards the formation of Pickering systems. Moreover, detailed stability analysis for emulsions should be applied. Overall, this study contributes to the existing understanding of the use of aquafaba as a plant-based functional ingredient, offering a sustainable alternative to traditional animal-derived and conventional hydrocolloids, while also opening avenues for the development of capsaicin-containing functional foods.

CRediT authorship contribution statement

S.S. Sahin: Conceptualization, Formal analysis, Investigation, Methodology, Writing – original draft, Writing – review & editing. **A.J. Hernández-Álvarez:** Investigation, Project administration, Supervision, Writing – review & editing. **L. Ke:** Investigation, Supervision, Writing – review & editing. **A. Sadeghpour:** Data curation, Formal analysis, Investigation, Writing – review & editing. **P. Ho:** Supervision, Writing – review & editing. **F.M. Goycoolea:** Conceptualization, Investigation, Project administration, Supervision, Writing – review & editing.

Declaration of competing interest

The authors declare that they have no known competing financial interests or personal relationships that could have appeared to influence the work reported in this paper.

Data availability

Data will be made available on request.

Acknowledgements

We acknowledge the doctoral scholarship from the Republic of Türkiye Ministry of National Education offered to Selvi Secil Sahin. The authors acknowledge Professor Michael Rappolt (University of Leeds) for his valuable contributions to the interpretation of the SAXS data.

Appendix A. Supplementary data

Supplementary data to this article can be found online at https://doi.org/10.1016/j.foodhyd.2024.109728.

References

Aengenheister, L., Dietrich, D., Sadeghpour, A., Manser, P., Diener, L., Wichser, A., et al. (2018). Gold nanoparticle distribution in advanced in vitro and ex vivo human placental barrier models. *Journal of Nanobiotechnology, 16*(1), 1–16. https://doi.org/10.1186/s12951-018-0406-6

Aguilera, Y., Esteban, R. M., Benítez, V., Mollá, E., & Martín-Cabrejas, M. A. (2009). Starch, functional properties, and microstructural characteristics in chickpea and lentil as affected by thermal processing. *Journal of Agricultural and Food Chemistry, 57*(22), 10682–10688. https://doi.org/10.1021/JF902042R

Akbas, E., Soyler, U. B., & Oztop, M. H. (2019). Physicochemical and antimicrobial properties of oleoresin capsicum nanoemulsions formulated with lecithin and sucrose monopalmitate. *Applied Biochemistry and Biotechnology, 188*, 54–71. https://doi.org/10.1007/s12010-018-2901-5

Alajaji, S. A., & El-Adawy, T. A. (2006). Nutritional composition of chickpea (Cicer arietinum L.) as affected by microwave cooking and other traditional cooking methods. *Journal of Food Composition and Analysis, 19*(8), 806–812. https://doi.org/10.1016/j.jfca.2006.03.015

Alsalman, F. B., & Ramaswamy, H. S. (2021). Evaluation of changes in protein quality of high-pressure treated aqueous aquafaba. *Molecules, 26*(1), 234. https://doi.org/10.3390/molecules26010234

Attia, R. S., Shehata, A. E. M., Aman, M. E., & Hamza, M. A. (1994). Effect of cooking and decortication on the physical properties, the chemical composition and the nutritive value of chickpea (Cicer arietinum L.). *Food Chemistry, 50*(2), 125–131.

Babick, F. (2019). Dynamic light scattering (DLS). In V.-D. Hodoroaba, W. E. S. Unger, & A. G. Shard (Eds.), *Characterization of nanoparticles* (pp. 137–172). Elsevier. https://doi.org/10.1016/B978-0-12-814182-3.00010-9.

Bar-El Dadon, S., Pascual, C. Y., Eshel, D., Teper-Bamnolker, P., Ibáñez, M. D. P., & Reifen, R. (2013). Vicilin and the basic subunit of legumin are putative chickpea allergens. *Food Chemistry, 138*(1), 13–18. https://doi.org/10.1016/j.foodchem.2012.10.031

Beaucage, G. (1996). Small-angle scattering from polymeric mass fractals of arbitrary mass-fractal dimension. *Journal of Applied Crystallography, 29*(2), 134–146. https://doi.org/10.1107/S0021889895011605

Bergmann, A. G. G. O., Fritz, G., & Glatter, O. (2000). Solving the generalized indirect Fourier transformation (GIFT) by Boltzmann simplex simulated annealing (BSSA). *Journal of Applied Crystallography, 33*(5), 1212–1216.

Blumenkrantz, N., & Asboe-Hansen, G. (1973). New method for quantitative determination of uranic acids. *Analytical Biochemistry, 54*(2), 484–489.

Buhl, T. F., Christensen, C. H., & Hammershøj, M. (2019). Aquafaba as an egg white substitute in food foams and emulsions: Protein composition and functional behavior. *Food Hydrocolloids, 96*, 354–364. https://doi.org/10.1016/j.foodhyd.2019.05.041

Cabrita, M., Simões, S., Álvarez-Castillo, E., Castelo-Branco, D., Tasso, A., Figueira, D., et al. (2023). Development of innovative clean label emulsions stabilized by vegetable proteins. *International Journal of Food Science and Technology, 58*(1), 406–422. https://doi.org/10.1111/IJFS.15963

Campos-Vega, R., Loarca-Piña, G., & Oomah, B. D. (2010). Minor components of pulses and their potential impact on human health. *Food Research International, 43*(2), 461–482. https://doi.org/10.1016/j.foodres.2009.09.004

Chang, Y. W., Alli, I., Konishi, Y., & Ziomek, E. (2011). Characterization of protein fractions from chickpea (Cicer arietinum L.) and oat (Avena sativa L.) seeds using proteomic techniques. *Food Research International, 44*(9), 3094–3104. https://doi.org/10.1016/j.foodres.2011.08.001

Crawford, K., Kerr, W., & Tyl, C. (2023). Effect of hydrocolloid addition on cake prepared with aquafaba as egg substitute. *International Journal of Food Science and Technology*. https://doi.org/10.1111/ijfs.16492

Crawford, K., Tyl, C., & Kerr, W. (2023). Evaluation of processing conditions and hydrocolloid addition on functional properties of aquafaba. *Foods, 12*(4), 775. https://doi.org/10.3390/foods12040775

da Silva Anthero, A. G., Moya, M. T. M. A., Torsoni, A. S., Cazarin, C. B. B., & Hubinger, M. D. (2022). Characterization of Capsicum oleoresin microparticles and in vivo evaluation of short-term capsaicin intake. *Food Chemistry X, 13*, Article 100179. https://doi.org/10.1016/j.fochx.2021.100179

de Almeida Costa, G. E., da Silva Queiroz-Monici, K., Reis, S. M. P. M., & de Oliveira, A. C. (2006). Chemical composition, dietary fibre and resistant starch contents of raw and cooked pea, common bean, chickpea and lentil legumes. *Food Chemistry, 94*(3), 327–330. https://doi.org/10.1016/j.foodchem.2004.11.020

Deep Singh, G., Wani, A. A., Kaur, D., & Sogi, D. S. (2008). Characterisation and functional properties of proteins of some Indian chickpea (Cicer arietinum) cultivars. *Journal of the Science of Food and Agriculture, 88*(5), 778–786. https://doi.org/10.1002/jsfa.3144

Dubois, M., Gilles, K. A., Hamilton, J. K., Rebers, P. A., & Smith, F. (1956). Colorimetric method for determination of sugars and related substances. *Analytical Chemistry, 28*(3), 350–356. https://pubs.acs.org/sharingguidelines.

Ercan, P., & El, S. N. (2016). Inhibitory effects of chickpea and Tribulus terrestris on lipase, α-amylase and α-glucosidase. *Food Chemistry, 205*, 163–169. https://doi.org/10.1016/j.foodchem.2016.03.012

Erem, E., Icyer, N. C., Tatlisu, N. B., Kilicli, M., Kaderoglu, G. H., & Toker, Ö. S. (2021). A new trend among plant-based food ingredients in food processing technology: Aquafaba. *Critical Reviews in Food Science and Nutrition, 63*(20), 4467–4484. https://doi.org/10.1080/10408398.2021.2002259

Frias, J., Vidal-Valverde, C., Sotomayor, C., Diaz-Pollan, C., & Urbano, G. (2000). Influence of processing on available carbohydrate content and antinutritional factors of chickpeas. *European Food Research and Technology, 210*(5), 340–345. https://doi.org/10.1007/S002170050560

Gao, G., Zhou, J., Jin, Y., Wang, H., Ding, Y., Zhou, J., et al. (2021). Nanoparticles derived from porcine bone soup attenuate oxidative stress-induced intestinal barrier injury in Caco-2 cell monolayer model. *Journal of Functional Foods, 83*, Article 104573. https://doi.org/10.1016/j.jff.2021.104573

Glatter, O. (1977). A new method for the evaluation of small-angle scattering data. *Journal of Applied Crystallography, 10*(5), 415–421.

Glatter, O. (2018). The inverse scattering problem. In *Scattering methods and their application in colloid and interface science* (pp. 33–77). Elsevier. https://doi.org/10.1107/s1600576718016023, 1.

Gopal, J., Muthu, M., Paul, D., Kim, D. H., & Chun, S. (2016). Bactericidal activity of green tea extracts: The importance of catechin containing nano particles. *Scientific Reports, 6*(1). https://doi.org/10.1038/srep19710

Grasso, N., Bot, F., Roos, Y. H., Crowley, S. V., Arendt, E. K., & O'Mahony, J. A. (2022). The influence of protein concentration on key quality attributes of chickpea-based alternatives to cheese. *Current Research in Food Science, 5*, 2004–2012. https://doi.org/10.1016/j.crfs.2022.09.028

Güçlü-Üstündağ, Ö., & Mazza, G. (2007). Saponins: Properties, applications and processing. *Critical Reviews in Food Science and Nutrition, 47*(3), 231–258. https://doi.org/10.1080/10408390600698197

Gumus, C. E., Decker, E. A., & McClements, D. J. (2017). Formation and stability of ω-3 oil emulsion-based delivery systems using plant proteins as emulsifiers: Lentil, pea, and faba bean proteins. *Food Biophysics, 12*, 186–197. https://doi.org/10.1007/s11483-017-9475-6

Guzmán, I., & Bosland, P. W. (2018). A matter of taste: Capsaicinoid diversity in Chile peppers and the importance to human food preference. In *Capsaicin and its human therapeutic development*. https://doi.org/10.5772/INTECHOPEN.77317. IntechOpen.

Han, H., Ke, L., Wang, H., Gao, G., Zhang, Y., Rao, P., et al. (2022). Incidental nanoparticles in black tea infusion: Carriers of bioactives fortifying protection on intestinal mucosal cells against oxidative stresses. *Food Biophysics, 17*(2), 209–220. https://doi.org/10.1007/s11483-021-09708-5

Han, I. H., Swanson, B. G., & Baik, B. K. (2007). Protein digestibility of selected legumes treated with ultrasound and high hydrostatic pressure during soaking. *Cereal Chemistry, 84*(5), 518–521. https://doi.org/10.1094/CCHEM-84-5-0518

Han, J., Zhang, S., Liu, X., & Xiao, C. (2020). Fabrication of capsaicin emulsions: Improving the stability of the system and relieving the irritation to the gastrointestinal tract of rats. *Journal of the Science of Food and Agriculture, 100*(1), 129–138. https://doi.org/10.1002/jsfa.10002

He, Y., Meda, V., Reaney, M. J. T., & Mustafa, R. (2021). Aquafaba, a new plant-based rheological additive for food applications. *Trends in Food Science & Technology, 111*, 27–42. https://doi.org/10.1016/j.tifs.2021.02.035

He, Y., Purdy, S. K., Tse, T. J., Tar'an, B., Meda, V., Reaney, M. J. T., et al. (2021). Standardization of aquafaba production and application in vegan mayonnaise analogs. *Foods, 10*(9), 1978. https://doi.org/10.3390/FOODS10091978

He, Y., Shim, Y. Y., Mustafa, R., Meda, V., & Reaney, M. J. T. (2019). Chickpea cultivar selection to produce aquafaba with superior emulsion properties. *Foods, 8*(12), 685. https://doi.org/10.3390/foods8120685

Kaiser, M., Higuera, I., & Goycoolea, F. M. (2017). Capsaicinoids: Occurrence, chemistry, biosynthesis and biological effects. In E. M. Yahia (Ed.), *Fruit and vegetable phytochemicals: Chemistry and human health* (2nd ed., pp. 499–514). John Wiley & Sons.

Kaiser, M., Kirsch, B., Hauser, H., Schneider, D., Seub-Baum, I., & Goycoolea, F. M. (2015). In vitro and sensory evaluation of capsaicin-loaded nanoformulations. *PLoS One, 10*(10). https://doi.org/10.1371/journal.pone.0141017

Kaiser, M., Lankamp, F., & Goycoolea, F. M. (2016). Nanoencapsulation of capsaicin attenuates the cytotoxic effect on Caco-2 cells. In P. A. Williams, & G. Phillips (Eds.), *Gums and stabilisers for the food industry 18: Hydrocolloid functionality for affordable and sustainable global food solutions* (pp. 176–181). Royal Society of Chemistry. https://doi.org/10.1039/9781782623830-fp001.

Karatay, G. G. B., Rebellato, A. P., Joy Steel, C., & Dupas Hubinger, M. (2022). Chickpea aquafaba-based emulsions as a fat replacer in pound cake: Impact on cake properties and sensory analysis. *Foods, 11*(16), 2484. https://doi.org/10.3390/FOODS11162484

Kaur, R., & Prasad, K. (2021). Technological, processing and nutritional aspects of chickpea (Cicer arietinum) - A review. *Trends in Food Science and Technology, 109*, 448–463. https://doi.org/10.1016/j.tifs.2021.01.044.

Kaur, S., Kaur, S., Gupta, A. K., & Kaur, J. (2016). Physiochemical and nutritional attributes of raw and soaked seeds of chickpea (Cicer arietinum L.) genotypes. *Legume Research, 39*(3), 359–369. https://doi.org/10.18805/lr.v0iOF.9434

Ke, L., Gao, G. Z., Shen, Y., Zhou, J. W., & Rao, P. F. (2015). Encapsulation of aconitine in self-assembled licorice protein nanoparticles reduces the toxicity in vivo. *Nanoscale Research Letters, 10*, 1–8. https://doi.org/10.1186/s11671-015-1155-1

Kim, J. H., Ko, J. A., Kim, J. T., Cha, D. S., Cho, J. H., Park, H. J., et al. (2014). Preparation of a capsaicin-loaded nanoemulsion for improving skin penetration. *Journal of Agricultural and Food Chemistry, 62*(3), 725–732. https://doi.org/10.1021/jf404220n

Kiselev, M. A., Janich, M., Hildebrand, A., Strunz, P., Neubert, R. H. H., & Lombardo, D. (2013). Structural transition in aqueous lipid/bile salt [DPPC/NaDC] supramolecular aggregates: SANS and DLS study. *Chemical Physics, 424*, 93–99. https://doi.org/10.1016/j.chemphys.2013.05.014

Krog, N. (2011). In J. W. Fuquay, P. F. Fox, & H. Roginski (Eds.), *Encyclopedia of Dairy Sciences (Second, 2* pp. 891–900). Academic Press.

Kumar, M., Tomar, M., Punia, S., Dhakane-Lad, J., Dhumal, S., Changan, S., et al. (2022). Plant-based proteins and their multifaceted industrial applications. *Lebensmittel-Wissenschaft und -Technologie, 154*, Article 112620. https://doi.org/10.1016/j.lwt.2021.112620

Laemmli, U. K. (1970). Cleavage of structural proteins during the assembly of the head of bacteriophage T4. *Nature, 227*(5259), 680–685.

Lake, J. A. (1967). An iterative method of slit-correcting small angle X-ray data. *Acta Crystallographica, 23*(2), 191–194.

Li, Y., Liu, X., Liu, H., & Zhu, L. (2022). *Interfacial adsorption behavior and interaction mechanism in saponin–protein composite systems: A review*. Food Hydrocolloids. https://doi.org/10.1016/j.foodhyd.2022.108295, 108295.

Lin, D., Lin, W., Gao, G., Zhou, J., Chen, T., Ke, L., et al. (2020). Purification and characterization of the major protein isolated from Semen Armeniacae Amarum and the properties of its thermally induced nanoparticles. *International Journal of Biological Macromolecules, 159*, 850–858. https://doi.org/10.1016/j.ijbiomac.2020.05.070

Liu, F., & Tang, C. H. (2016). Soy glycinin as food-grade Pickering stabilizers: Part. III. Fabrication of gel-like emulsions and their potential as sustained-release delivery systems for β-carotene. *Food Hydrocolloids, 56*, 434–444. https://doi.org/10.1016/j.foodhyd.2016.01.002

López-Franco, Y. L., de la Barca, A. M. C., Valdez, M. A., Peter, M. G., Rinaudo, M., Chambat, G., et al. (2008). Structural characterization of mesquite (Prosopis velutina) gum and its fractions. *Macromolecular Bioscience, 8*(8), 749–757. https://doi.org/10.1002/mabi.200700285

McClements, D. J. (2005). Characterization of emulsion properties. In F. M. Clydesdale (Ed.), *Food emulsions principles, practices, and techniques* (2nd ed., pp. 461–512). CRC Press.

Meurer, M. C., de Souza, D., & Marczak, L. D. F. (2020). Effects of ultrasound on technological properties of chickpea cooking water (aquafaba). *Journal of Food Engineering, 265*, Article 109688. https://doi.org/10.1016/j.jfoodeng.2019.109688

Morton, P. A. J., & Murray, B. S. (2001). Acid beverage floc: Protein-saponin interactions and an unstable emulsion model. *Colloids and Surfaces B: Biointerfaces, 21*(1–3), 101–106. www.elsevier.nl/locate/colsurfb.

Mustafa, R., He, Y., Shim, Y. Y., & Reaney, M. J. T. (2018). Aquafaba, wastewater from chickpea canning, functions as an egg replacer in sponge cake. *International Journal of Food Science and Technology, 53*(10), 2247–2255. https://doi.org/10.1111/ijfs.13813

Mustafa, R., & Reaney, M. J. T. (2020). Aquafaba, from food waste to a value-added product. *Food Wastes and By-products: Nutraceutical and Health Potential*, 93–126. https://doi.org/10.1002/9781119534167.ch4

Nicoli, M. C., Anese, M., & Parpinel, M. (1999). Influence of processing on the antioxidant properties of fruit and vegetables. *Trends in Food Science & Technology, 10*(3), 94–100.

Papalamprou, E. M., Doxastakis, G. I., Biliaderis, C. G., & Kiosseoglou, V. (2009). Influence of preparation methods on physicochemical and gelation properties of chickpea protein isolates. *Food Hydrocolloids, 23*(2), 337–343. https://doi.org/10.1016/j.foodhyd.2008.03.006

Peter, K. V., & Babu, K. N. (2012). Introduction to herbs and spices: Medicinal uses and sustainable production. In K. V. Peter (Ed.), *Handbook of herbs and spices* (pp. 1–16). Woodhead Publishing.

Pico, J., Pismag, R. Y., Laudouze, M., & Martinez, M. M. (2020). Systematic evaluation of the Folin-Ciocalteu and Fast Blue BB reactions during the analysis of total phenolics in legumes, nuts and plant seeds. *Food & Function, 11*(11), 9868–9880. https://doi.org/10.1039/d0fo01857k

Potter, S. M., Jimenez-Flores, R., Pollack, J., Lone, T. A., & Berber-Jimenez, M. D. (1993). Protein-saponin interaction and its influence on blood lipids. *Journal of Agricultural and Food Chemistry, 41*(8), 1287–1291. https://pubs.acs.org/sharingguidelines.

Raikos, V., Hayes, E. H., Agriopoulou, S., & Varzakas, T. (2020a). Proteomic dataset of aquafaba from canned chickpea (Cicer arietinum L.) broth. *Current Topics in Peptide & Protein Research, 21*, 61–68.

Raikos, V., Hayes, H., & Ni, H. (2020b). Aquafaba from commercially canned chickpeas as potential egg replacer for the development of vegan mayonnaise: Recipe optimisation and storage stability. *International Journal of Food Science and Technology, 55*(5), 1935–1942. https://doi.org/10.1111/ijfs.14427

Ren, Z., Chen, Z., Zhang, Y., Lin, X., & Li, B. (2019). Novel food-grade Pickering emulsions stabilized by tea water-insoluble protein nanoparticles from tea residues. *Food Hydrocolloids, 96*, 322–330. https://doi.org/10.1016/j.foodhyd.2019.05.015

Ruiz, R. G., Price, K. R., Arthur, A. E., Rose, M. E., Rhodes, M. J. C., & Fenwick, R. G. (1996). Effect of soaking and cooking on the saponin content and composition of chickpeas (cicer arietinum) and lentils (lens culinaris). *Journal of Agricultural and Food Chemistry, 44*(6), 1526–1530.

Ryan, K. N., Vardhanabhuti, B., Jaramillo, D. P., van Zanten, Coupland, J. N., & Foegeding, E. A. (2012). Stability and mechanism of whey protein soluble aggregates thermally treated with salts. *Food Hydrocolloids, 27*(2), 411–420. https://doi.org/10.1016/j.foodhyd.2011.11.006.

Sadeghpour, A., Pirolt, F., & Glatter, O. (2013). Submicrometer-sized Pickering emulsions stabilized by silica nanoparticles with adsorbed oleic acid. *Langmuir, 29*(20), 6004–6012. https://doi.org/10.1021/la4008685

Sánchez-Mata, M. C., Peñuela-Teruel, M. J., Cámara-Hurtado, M., Díez-Marqués, C., & Torija-Isasa, M. E. (1998). Determination of mono-, di-, and oligosaccharides in legumes by high-performance liquid chromatography using an amino-bonded silica column. *Journal of Agricultural and Food Chemistry, 46*(9), 3648–3652. https://doi.org/10.1021/JF980127W

Sánchez-Velázquez, O. A., Ribéreau, S., Mondor, M., Cuevas-Rodríguez, E. O., Arcand, Y., & Hernández-Alvarez, Á. J. (2021). Impact of processing on the in vitro protein quality, bioactive compounds, and antioxidant potential of 10 selected pulses. *Legume Science, 3*(2). https://doi.org/10.1002/leg3.88

Sarkar, A., & Dickinson, E. (2020). Sustainable food-grade Pickering emulsions stabilized by plant-based particles. *Current Opinion in Colloid & Interface Science, 49*, 69–81. https://doi.org/10.1016/j.cocis.2020.04.004

Sathyanarayana, S., & Prashanth, K. V. H. (2019). Malting process has minimal influence on the structure of arabinan-rich rhamnogalacturonan pectic polysaccharides from chickpea (Cicer arietinum L.) hull. *Journal of Food Science and Technology, 56*(4), 1732–1743. https://doi.org/10.1007/s13197-019-03600-4

Shevkani, K., Singh, N., Chen, Y., Kaur, A., & Yu, L. (2019). Pulse proteins: Secondary structure, functionality and applications. *Journal of Food Science and Technology, 56*, 2787–2798. https://doi.org/10.1007/S13197-019-03723-8

Shim, Y. Y., Mustafa, R., Shen, J., Ratanapariyanuch, K., & Reaney, M. J. T. (2018). Composition and properties of aquafaba: Water recovered from commercially canned chickpeas. *Journal of Visualized Experiments, 132*, Article e56305. https://doi.org/10.3791/56305

Singh, B., Singh, J. P., Singh, N., & Kaur, A. (2017). Saponins in pulses and their health promoting activities: A review. *Food Chemistry, 233*, 540–549. https://doi.org/10.1016/j.foodchem.2017.04.161

Singleton, V. L., Orthofer, R., & Lamuela-Raventós, R. M. (1999). Analysis of total phenols and other oxidation substrates and antioxidants by means of folin-ciocalteu reagent. *Methods in Enzymology, 299*, 152–178.

Siva, N., Thavarajah, P., Kumar, S., & Thavarajah, D. (2019). Variability in prebiotic carbohydrates in different market classes of chickpea, common bean, and lentil collected from the American local market. *Frontiers in Nutrition, 6*, 38. https://doi.org/10.3389/fnut.2019.00038

Srivastava, R. P., & Vasishtha, H. (2013). Soaking and cooking effect on sapogenols of chickpeas (Cicer arietinum). *Current Advances in Agricultural Sciences, 5*(1), 141–143. https://www.researchgate.net/publication/256078874.

Stantiall, S. E., Dale, K. J., Calizo, F. S., & Serventi, L. (2018). Application of pulses cooking water as functional ingredients: The foaming and gelling abilities. *European Food Research and Technology, 244*, 97–104. https://doi.org/10.1007/S00217-017-2943-X/TABLES/4

Su, J., Guo, Q., Chen, Y., Dong, W., Mao, L., Gao, Y., et al. (2020). Characterization and formation mechanism of lutein Pickering emulsion gels stabilized by β-lactoglobulin-gum Arabic composite colloidal nanoparticles. *Food Hydrocolloids, 98*. https://doi.org/10.1016/j.foodhyd.2019.105276

Sukhotu, R., Guo, S., Xing, J., Hu, Q., Wang, R., Shi, X., et al. (2016). Changes in physiochemical properties and stability of peanut oil body emulsions by applying gum Arabic. *Lebensmittel-Wissenschaft und -Technologie, 68*, 432–438. https://doi.org/10.1016/j.lwt.2015.12.055

The Official Aquafaba Website. (2016). *Aquafaba history*. http://aquafaba.com/.

Tosh, S. M., Farnworth, E. R., Brummer, Y., Duncan, A. M., Wright, A. J., Boye, J. I., et al. (2013). Nutritional profile and carbohydrate characterization of spray-dried lentil, pea and chickpea ingredients. *Foods, 2*(3), 338–349. https://doi.org/10.3390/foods2030338

Tufaro, D., & Cappa, C. (2023). Chickpea cooking water (Aquafaba): Technological properties and application in a model confectionery product. *Food Hydrocolloids, 136*. https://doi.org/10.1016/j.foodhyd.2022.108231

UniProtKB. (2004a). Arietin - cicer arietinum (chickpea) | UniProtKB | UniProt. https://www.uniprot.org/uniprotkb/P83988/entry.

UniProtKB. (2004b). Cicerin - cicer arietinum (chickpea) | UniProtKB | UniProt. https://www.uniprot.org/uniprotkb/P83987/entry#names_and_taxonomy.

Vallverdú-Queralt, A., Regueiro, J., Rinaldi de Alvarenga, J. F., Torrado, X., & Lamuela-Raventos, R. M. (2014). Home cooking and phenolics: Effect of thermal treatment and addition of extra virgin olive oil on the phenolic profile of tomato sauces. *Journal of Agricultural and Food Chemistry, 62*(14), 3314–3320. https://doi.org/10.1021/jf500416n

Wood, J. A., Knights, E. J., & Choct, M. (2011). Morphology of chickpea seeds (Cicer arietinum l.): Comparison of Desi and Kabuli types. *International Journal of Plant Sciences, 172*(5), 632–643. https://doi.org/10.1086/659456

Wu, X., Xu, N., Cheng, C., McClements, D. J., Chen, X., Zou, L., et al. (2022). Encapsulation of hydrophobic capsaicin within the aqueous phase of water-in-oil high internal phase emulsions: Controlled release, reduced irritation, and enhanced bioaccessibility. *Food Hydrocolloids, 123*, Article 107184. https://doi.org/10.1016/j.foodhyd.2021.107184

Xiao, J., Wang, X., Gonzalez, A. J. P., & Huang, Q. (2016). Kafirin nanoparticles-stabilized Pickering emulsions: Microstructure and rheological behavior. *Food Hydrocolloids, 54*, 30–39. https://doi.org/10.1016/j.foodhyd.2015.09.008

Xiaoli, X., Liyi, Y., Shuang, H., Wei, L., Yi, S., Hao, M., et al. (2008). Determination of oligosaccharide contents in 19 cultivars of chickpea (Cicer arietinum L) seeds by high performance liquid chromatography. *Food Chemistry, 111*(1), 215–219. https://doi.org/10.1016/j.foodchem.2008.03.039

Xie, J. H., Shen, M. Y., Nie, S. P., Liu, X., Zhang, H., & Xie, M. Y. (2013). Analysis of monosaccharide composition of Cyclocarya paliurus polysaccharide with anion exchange chromatography. *Carbohydrate Polymers, 98*(1), 976–981. https://doi.org/10.1016/j.carbpol.2013.07.011

Xu, Y., Cartier, A., Obielodan, M., Jordan, K., Hairston, T., Shannon, A., et al. (2016). Nutritional and anti-nutritional composition, and in vitro protein digestibility of Kabuli chickpea (Cicer arietinum L.) as affected by differential processing methods. *Journal of Food Measurement and Characterization, 10*, 625–633. https://doi.org/10.1007/s11694-016-9346-8

Xu, Y., Obielodan, M., Sismour, E., Arnett, A., Alzahrani, S., & Zhang, B. (2017). Physicochemical, functional, thermal and structural properties of isolated Kabuli chickpea proteins as affected by processing approaches. *International Journal of Food Science and Technology, 52*(5), 1147–1154. https://doi.org/10.1111/ijfs.13400

Yu, B., Patterson, N., & Zaharia, L. I. (2022). Saponin biosynthesis in pulses. *Plants, 11*(24), 3505. https://doi.org/10.3390/plants11243505

Zhao, Q., Wang, L., Hong, X., Liu, Y., & Li, J. (2021). Structural and functional properties of perilla protein isolate extracted from oilseed residues and its utilization in Pickering emulsions. *Food Hydrocolloids, 113*, Article 106412. https://doi.org/10.1016/j.foodhyd.2020.106412

Zhao, Z., Wang, W., Xiao, J., Chen, Y., & Cao, Y. (2020). Interfacial engineering of pickering emulsion Co-stabilized by zein nanoparticles and tween 20: Effects of the particle size on the interfacial concentration of gallic acid and the oxidative stability. *Nanomaterials, 10*(6), 1068. https://doi.org/10.3390/nano10061068